# Journal of ISAS

An open access peer reviewed quarterly e-journal by
## Indian Society of Analytical Scientists

# Journal of ISAS

An open access peer reviewed quarterly e-journal published by Indian Society of Analytical Scientists

President ISAS : Dr. P.P.Chandrachoodan

J.ISAS

Cover page images- curtsey Pixabay.com

# Instruction to Authors

- The Manuscript should be typed in **MS word** (times new roman) with **1.5 spacings** and **font size 12**
- The **title** of the paper should be clear and concise(**font size 14 and bold**), the first letter of each noun and adjective in the title must be in capital letter. It will be followed by names of authors(initials followed by surname) with their affiliation ( **font size 12)**
- Corresponding author should be indicated by * with email ID
- The text should be divided into following sections:
- **Abstract : up to 300 words**
- **Key words: 5-6**
- **Introduction**
- **Experimental**
- **Results and Discussion**
- **Conclusions**
- **Acknowledgement**
- Figures and Tables should be before references with a caption **Figures:** Followed by **Tables:**
- **References**

- Divisions within the section should be indicated as subheadings
- The figures and tables should be numbered with Roman numerals and must be mentioned in the text at appropriate places
- Standard abbreviations for technical terms and journals should be used
- All constants should be expressed in **SI units**
- References should be numbered consecutively and should appear in the text as superscript at appropriate places.
- References should be in following pattern
  **For research paper**:
  Authors' initials and surname, Journal abbreviation, Volume, Page, Year.
  **For book**:
  Authors' initials and surname, Book name, Publisher, Place, Year.
  **For proceedings**:
  Authors' initials and surname Proceedings' of the conference name, place, Page, Month and Year.

- The paper is to be submitted in word file and PDF file to isasjournal@isasbharat.in
- After getting the acceptance of the paper, authors have to submit **signed copyright form  and undertaking** before publishing the article

# ISAS

Indian Society of Analytical Scientists.



## Editorial

After an enthusiastic response to inaugural issue of Journal of ISAS, we are bringing out the second issue of our journal with reviews, research articles and short communication  It contains an exhaustive review on applications of nanoparticles in medicine along with other research articles wherein various techniques have been used as an analytical tool to explore research in different fields, at the end a short review on "Nuclear Analytical Techniques" booklet is included.  I assure you that "Journal of ISAS" will be always innovative providing a special space for scholarly works representing the integration of all branches of science.

I would like to express my sincere gratitude towards Dr. P.P. Chandrachoodan, President ISAS; Dr. Raghaw Saran, Vice president ISAS and Chairman, Advisory board of Journal of ISAS for their guidance, inspiration and support at each stage of journal progress. I wish to express my special thanks to Editorial board members: Dr.  Vijayalaxmi Adya and Dr. Vinay Bhandari for their continuous cooperation. Cooperation from  Editorial and Advisory board members and reviewers is gratefully acknowledged. I congratulate all the contributory authors for their  articles in this issue. My sincere thanks are due  to Kailash Gharat, Shivani Kantak, Vaibhav Parse and Smruti Adya for  their technical support.

I invite all ISAS Members from different parts of our country to go through both the volumes and contribute towards forthcoming issues along with their colleagues and students.

Looking forward for your response and articles in future issue.

Dr. Nilima Rajurkar
Editor in Chief
Journal of ISAS

..

# Journal of ISAS

## 1(2), Pages 1 to 84, (2022)

## Contents

# Application of Nanoparticles in Medicine

**Maharshi Pandya and Raghaw Saran**[*]
**RKNEC, Nagpur**
***Email: saranraghaw@gmail.com**

**Abstract**

Nanomaterials due to their size (ranging from 0.1-100 nm, at least in one dimension) and higher ratio of surface area to volume display dominant quantum effects causing drastic changes in their chemical reactivity as well as optical, elastic, electrical and magnetic properties. The electrons due to their wave nature move very easily without scattering in nanomaterials and allow their use as biological sensors. Nano wires, semiconducting in nature, act as a versatile optoelectronic component in photodetectors sensitive to polarization and arrays with sub wavelength resolution. The wide applicability of nanomaterials in medicines emerge from the similarity in size of biomolecule moieties of metabolic processes occurring at nano levels.

Optical properties of quantum dots allow their use as biomarkers subsequent to coating with a material able to bind selectively with certain biological structures like cancer cells by fluorescent absorption followed by emission of electrons known as functionalised quantum dots. Nanomaterials on combining with biomolecules develop ability to recognize sensitive diagnostic and regulated drug delivery processes with appreciably better performances and may be used as tissue substitutes. The properties produced in organic solvents make them hydrophobic and incompatible to biological molecules. At the same time, they may be converted into water soluble form and made biocompatible through different techniques like ligand exchange, encapsulation, polymer coating (with functional groups attached to the surface) providing reactive site for bio conjugation through different processes keeping limitations of the processes in view.

Nanomaterials play prominent role in medicines as obviated by growing global market for them in the field expected to reach to USD 182.3 billion by 2027 at a compounded annual growth rate of 19.9% from 2021.

**Keywords**: Nanomaterials, Quantum effect, Drug delivery, Cancer, Characterization, Limitations

**Introduction**

Nanomaterials (NM), (size ranging from 0.1-100 nm, at least in one dimension)[1,2] have relatively appreciable fractions of large number of atoms on the surface making quantum effect dominant altering chemical reactivity as well as optical, elastic, electrical and magnetic properties drastically. Furthermore, wave nature of electrons in nanomaterials has far reaching consequences on electronic energy levels and electrical properties in zero, one- and two-dimensional nanostructures. Electrons in graphene move very easily without scattering and may be used as biological sensors. Semiconducting nano wires act as a versatile optoelectronic component in polarization sensitive photodetectors and arrays with sub wavelength resolution.

Optical properties of functionalised (coated) quantum dots allow their use as biomarkers subsequent to coating with a material able to bind selectively with certain biological structures like cancer cells. The coated dots have usually CdS, CdSe, and CdTe as core material with ZnS as fluorescent coat. Cancer cells are identified by fluorescent absorption followed by emission of electrons.

Biomolecules on combining with NM develop unique characteristics due to their properties of recognizing sensitive diagnostic and regulated drug delivery implements with appreciably better performances and may be used as novel tissue substitutes, NMs can be divided according to their geometry such as equiaxed (equal in all dimensions), one dimensional (fibrous or wire) and two-dimensional or lamellar. The physical, electronic, chemical and optical properties as well as unique quantum mechanical effects of NM, give rise to unexpected physicochemical properties. The properties produced in organic solvents make them hydrophobic and incompatible to biological molecules. At the same time, they may be converted into water soluble form to make them biocompatible through different techniques. The techniques include ligand exchange, encapsulation, polymer coating (with functional groups attached to the surface) and provide reactive site for bio conjugation or cross linking through direct attachment (hydrophobic or electrostatic interaction) and some time through biotin avidin systems. The molecules produced have to be checked for drawbacks like low yield and loss of functionality after conjugation.

The NM biosensors are highly sensitive, stable, assembled into barcodes and high-density arrays needing light emitting diodes as power source. Researches in Nanotechnology leads to miniaturized, speedier, automated, less error prone, disposable devices for the analysis of genetic structure; their effect on cellular functions changes focus from diagnosis and

treatment to identification and prevention. This leads to individually tailored patients' specific treatment and therapies.

## Requisites of Nanomaterials

Quantum dots (QDs) fluorescence exhibits broad excitation profile, narrow and symmetric emission spectra, high photo stability, high quantum efficiency and excellent multiple detection capability    in biosensing[3] and imaging contrary to organic dyes. Near- field scanning optical microscope (NSOM) has helped in developing nano transducers which recognize the binding events and actively generate highly sensitive signals simultaneously. NM for drug delivery to tumours, must be small (<100 nm), nontoxic, should not aggregate, should be biodegradable and biocompatible. They should avoid the reticulo-endothelial system (RES) uptake[4], should not aggregate, escape opsonization, be non-inflammatory besides prolonged circulation time to make the drug more effective for therapy and should be economic cost wise, with minimum side effect. Effects of size, charge, shape, surface modification, loading and other chemical properties of NM on the drug delivery system while employing it as carrier need to be examined.  Besides, Interaction of NM with their hosts in bio distribution, organ accumulation/ degradation, toxicity, genetic or cellular structure damage or inflammatory foreign body effect, toxicity of nanocarriers and various other parameters need to be investigated.

## Benefits of Nanomaterials

Nanoparticles, their nano-range size at least in one dimension, with a small diameter of 0.1-1000 nm in general, in medicine 5-250 nm[5] and a very high surface area to volume ratio render their high reliability and reproducibility[6] in drug delivery. An industrial revolution is in offing in nanoscience, to convert negative nanostructures into its positive and productive aspect. Nanotechnology is predicted to play a great role in the developing world, contributing to advances in medicine and pharmacy besides transport, energy storage etc[7]. Their shape, surface properties and size on modification give rise to several nano systems which may be utilized in imaging, diagnosis and treatment of serious diseases. Besides, they may also be utilised in dentistry, sunscreens, cosmetics, environmental clean-up, gene inactivation and biological sensors[8,9,10].

The nano materials with characteristic functional groups at the nano scale, prepared by physical and chemical methods, send drugs to particular sites or tissues[11]. Tissue and cell interactions are function of several parameters such as charge, size, shape and structure of

drug molecules[12] which may be optimized by studying and regulating them. Nanotechnology products find extensive use in healthcare. Several nano systems have been developed for prevention, identification, deciphering and cure of several diseases such as cancer, cardiovascular, ocular and central nervous system related diseases[13,14,15.] Several nano systems have been revealed to be more efficient in comparison to conventional ones for theragnostic (therapeutic and diagnostic both) purposes. The radioactive drugs are used to diagnose and drug delivers therapy to treat the main and any metastatic tumours.

Nano materials gel with biomedical devices due to their almost similar sizes[9]. In the field of drug delivery, nano systems render the drug supply with high degree of precision to the target at a regulated rate increasing delivery time in comparison to usual processes.

Nano particles are highly effective in drug delivery to the specific target locations utilizing biodegradable materials in the majority of the cases[16,17]. The drug delivery is further facilitated due to their ability to cross blood brain barrier entering pulmonary system, endothelium of tumours coupled with absorption through tight junctions of skin endothelial cells. The effective absorption by different types of cells as well as selective drug delivery in the target locations[18,19] make the nano particles of immense use in drug delivery system. Their small particle size and large surface area[20] cause greater solubility and superior bioavailability. The active pharmaceutical ingredients (API) are dissolved, entrapped, encapsulated or linked to nanoparticle matrix[21]. Nanoparticles may be utilized to transport proteins, nucleic acid, antibiotics, vaccines besides their use as drug delivery systems in different type of therapies such as gene therapy, cancer therapy, aids therapy etc.

Nanoparticles may also be used more efficiently for intravenous administration than conventional micro-particles. Due to their relatively smaller size than that of the smallest body capillaries (diameter 5-6 µm) they are free from causing obstruction in an artery, by a clot of blood or an air bubble i.e., embolism. Natural and synthetic biodegradable polymer may be used for preparation of Nanoparticles with improved bioavailability and controlled release behaviour of medicines in a particular dose at a focal point for an elongated duration by adapting the system in a way to prevent endogenous system to destroy the drug[22]. Moreover, Nanoparticles act as creative carrier systems for proteins or nucleic acids present in medicines (even without proper formulation) to avoid their decomposition and improve their efficiency[23].

**Types of Nanoparticles used in Medicine**
**Carbon nanotubes (CNT)**

Carbon nanotubes are nanosized, seamless carbon-based tubular structures constituted of graphite cylindrical sheets, sealed at one or both ends by bucky balls of varying length from 1 to 100 nm. They may be single or multiwalled nanotubes (SWNT or MWNT) suitable for detection of DNA mutation as diameter of DNA helix is half the size of SWNT. On the contrary, diameter of MWNT varies according to the number of walls in their structure and extend from a few nm to tens of nanometers[24]. Nanotubes possess the unique feature of entering living cell without causing its death or any other damage. It appears they behave like miniaturized needles and enter cells spontaneously with unrecognised mechanism. As revealed by computer simulation, the CNT are absorbed and accommodated onto the membrane surface with their axis parallel to plane of membrane. Cells don't recognize them as harmful intruder due to their smaller size (diameter 2-50 nm about 10,000 to 50, 000 smaller than human hair). The use of CNTs in drug delivery requires attachment of different functional groups on the external surface of nanotubes. The modified CNTs are used for delivery of antibiotics to different types of cells by selective transport through the membrane. CNT were used in administration of amphotericin -B a very powerful antibiotic considered to be most effective in chronic fungal diseases[25]. CNT finds use as a vector in gene delivery. Hollow core of CNT permits encapsulation of molecules.

CNT and fullerenes ($C_{60}$, $C_{70}$, $C_{76}$ etc., found in variety of graphite cylinder with hollow cage like configurations suitable for drug encapsulation) used as drug transporters are generally, produced by chemical vapour deposition, combustion procedures and electric arc discharge. Their capability is characterised by the strength and stability of the structures of nanotubes and fullerenes, CNTs being one of the strongest materials in terms of tensile strength and modulus of elasticity (almost 100 times of steel) due to covalent $sp^2$ bond existing between individual C atoms. They were also shown to exhibit antioxidant and antimicrobial activity[26]. The structure of fullerenes was capable of targeting tissues and intracellular mitochondria. CNT with their capability to cross partially permeable cell membrane very easily have potential to overcome obstructions, impossible to remove at an early stage, and therefore, find wide application in modern healthcare systems. Their capability to carry small molecules such as organic drugs, proteins, peptides, nucleic acids, antibiotics, etc., enhances further their utility. The molecules may be carried to precise location forming covalent bonds, adsorption or encapsulation in the CNT. Covalent or non -covalent bonding of smaller proteins (less than 80 KDa) with CNT help them in getting absorbed by smaller cells

covalently or non-covalently and are engulfed within the cell membrane via endocytosis[27]. X-rays produced from CNT (cold X-rays) allow imaging of superior quality due to its properties. The cells containing CNT solution on exposure to a laser infrared beam doesn't get destroyed despite getting heated up to 158° F up to two minutes due to CNT absorbing near infrared waves. Cancer cells, other than the normal cells, absorb wavelengths, and may be killed effectively by laser (with appropriate wavelength) due to their high intensity and near monochromaticity.

CNT are extensively used in treatment of osteoporosis, broken bones, blood compatible heparin CNT as artificial kidney[28], as heparin composite membrane with nano-pores could work efficiently as an artificial kidney (dialyzer) by filtering the blood and maintaining its flow. However, dispersion of CNT with tendency to aggregate in large bundles and ropes (due to their higher molecular weight and strong intertubular force (Vander Walls and electrostatics) specially in saline media or serum commonly used in toxicology, dictating entry into cell significantly, poses a big limitation. Sonification, use of surfactant in aqueous solution or highly polar organic solvents such as N, N dimethylformamide along with ultrasonic baths or probes gives stable dispersion in individual pristine CNT[27]. Many toxicological findings still consist of CNT aggregate. Chemical functionalisation i.e., covalently attaching appropriate molecules like peptides, acids, amines, polymers and poly-L- lysine to the side walls of CNT, most commonly achieved by amidation or esterification of the COOH group present after CNT purification or adsorption of bio molecules (most promising dispersion technique).

**Quantum dots**

Quantum dots (QD) nano crystals of size between 1.5- 10 nm are made up of semi-conducting structures. Their inorganic semiconductor nature allows electrons to transport enabling QD to fluoresce, emit different colours of light[29] according to their size (due to scattering). The phenomenon enables their use as labels in biosensing and imaging making them highly advantageous over the conventional organic dyes, due to their ability to emit several wavelengths on excitation with a single source as against organic dyes which need several excitation sources to emit different wavelengths. QD could therefore, be efficiently exploited to identify multiple targets as fluorescent probe other than the normal cells simultaneously, leading to replacement of organic dyes. Furthermore, they show high quantum efficiency, high stability to excitation and exceptional multiplexed detection capability[30, 31].

QD are inorganic semiconductor nano crystals. The core is constituted of CdSe, CdTe and CdS with an organic shell covered with a layer of ZnS to make them luminescent on exposure to light. Solubility of QD improves in aqueous buffer by adding a cap to QD[32]. QD prepared from heavy metals like Cd are highly toxic and carcinogenic and therefore, avoided in health care. On the contrary, graphene and carbon QD have wide scope in health sector[33] as they are stable and safe. Some of the uses of QD in diagnostic and therapeutic applications include cell labelling, DNA hybridisation, creation of non- viral vectors for gene therapy, biomolecule detection and biological performance and act as carrier for drugs utilised for cancer cure. They also convey biological and non- biological agents[34] and act as carriers for cancer treatment. Semiconducting nano-materials ZnO, CuO and $TiO_2$ are mostly used in drug delivery.

**Nanoshells**

Nanoshells comprising of economic dielectric silica core with an outer metallic thin layer (usually gold) are used to target drugs after adequate alterations. The alterations cause varying characteristics with variations in ratio between the core and the shell. The Nanoshells are used to cover particles of specific shape to achieve desired morphology.

They are inexpensive as precious metals can be added to the dielectric economic cores and thus amount of precious metals is required in smaller quantities during synthesising nanoshells[35] for example gold nanoshells. The targeting efficacy of nanoshells is enhanced towards cancer cell due to antibodies occupying their outer gold surface[36].

**Nanobubbles**

Nanobubbles or ultrafine bubbles are cavities of gases with diameter less than 200 nm[37]. They are formed at the interface of lipophilic surfaces in liquids by cavitation process, mix at body temperature and form larger microbubbles by rapid dissolution of the supersaturated liquid. Microbubbles are stable at room temperature and rise up in supersaturated solution due to gas nucleation at the hydrophobic surface and cause air gas trapping. The nanobubbles may be classified as plasmonic, bulk, oscillating and interfacial Nanobubbles and on loading with drugs effectively target tumour tissues and thus have high utility for cancer treatment. The uptake of tumour cells by Nanobubbles is appreciably enhanced when exposed to ultrasound[38, 39].

Basically, microbubbles (sort of gas-liquid emulsions) have core of an inert gas surrounded by a protective biocompatible shell (of lipids, albumin, protein or polymer). The shell protects leakage of gas and particle fusion[40]. Diameter of the shell ranges between 1-10 µm

with varying shell compositions. Elasticity of the material depends on the shell composition. Higher the elasticity of the material greater the acoustic energy microbubble may withstand. Microbubbles loaded with an active drug being lipophilic can easily penetrate through brain, blood barrier (BBB) and deliver the drug into brain tissue through a focused ultrasound which ruptures tight junctions in a particular localized area and increases permeability[41] of BBB.

Microbubble combined with ultrasound helps in diagnostic applications as well as therapeutics to different lesions. Tumours due to leaky vasculature have large gaps of about 700 nm between the endothelial cells, provide access to nanoparticles of size less than 700 nm[42]. Nanobubbles similar to micro bubbles act as a promising agent for imaging and/ or therapeutic use.

MRI coupled with ultrasound therapy is utilised in a non-invasive thermal ablation method for the cure of uterine fibroids. The method has approval of FDA. The method is also used as a treatment for liver, bone prostrate and brain related diseases[43, 44].

**Paramagnetic Nanoparticles**

Paramagnetic Nanoparticles (PN) are small particles with diameter slightly less than 100 nm. They could be prepared by applying strong magnetic fields to paramagnetic substances i.e., atoms with unpaired electrons (gadolinium, magnesium, lithium, tantalum etc.). PN are classified on the basis of their magnetic sensitivity. PN have higher magnetic susceptibility. Under the influence of a magnetic field, PN act as effective targets for identification of specific organs[45,46]. They mainly comprise of rare earth metal oxides and hydroxides. The most commonly used rare earth is $Gd^{3+}$ due to maximum number of unpaired electrons present in it (or $Mn^{2+}$) and is used as a positive contrast agent for MRI to improve the quality and hence accuracy of diagnosis of MRI scan

**Liposomes**

Liposomes are spherical double layered vesicles surrounding an aqueous core domain of the size varying from 50 nm to several micrometers. Liposome, synthetic particles, self-assembled amphiphilic phospholipids are in general, biocompatible as well as biodegradable with reduced toxicity and systemic effects[47]. Modified nanoscale liposomes are employed for transfer of proteins, DNA, small interferant (si) RNA, and cancer treatment but suffer from limitations of incapability to penetrate cells[48] causing discharge of drugs into extra cellular fluid besides rapid and inability to regulate[49] drug release and low loading capacity. However, drugs may be trapped persistently in aqueous phase of liposome with minimum drug loss during circulation[50] by using ammonium sulphate and may be coupled with antibodies to deliver drug to specific target[51].

**Niosomes**

Niosomes, with unique characteristics of containing lipophilic and lipophobic both agents[52] can be utilized as a new delivery system of drugs. They are self-assembled cluster of non-ionic surfactant molecules in aqueous phase. Their entrapment volume is decreased during formulation due to intercalation of cholesterol in their bilayers reducing their entrapment efficiency[53]. However, currently they are adopted for delivery of potent drugs[54] due to their entrapment capability to a broad extent for treatment of cancer[55] and viral diseases[54]. In vivo niosomes behave similar to liposome in extending entrapped drug circulation and may replace liposome as they are highly stable as well as nontoxic.

**Dendrimers**

Dendrimers with a small size in the range of 1-10 nm, 3D globules with branched layers giving rise to spherical shape create voids useful to entrap drugs and consequent delivery. They are biodegradable nanopolymers. Due to their lipophilic nature and small size, they can penetrate through cell membrane and are used for delivery of genes, drugs and vaccination. They are special category of polymers characterized by their core, made of an atom or multifunctional molecule, repeated branching bonded to the core usually covalently with functional groups at free ends to be conjugated to other molecules[56] and surface. Dendrimers interact chemically either through ionizable functional groups or through covalent bonding subsequent to mixing of their surface with active functional groups such as p- aminobenzoic acid, poly ethylene glycol (PEG) etc., formation of covalent bonds with the functional groups allows conjugation of dyes with dendrimers. Highly selective nature of dendrimers to target the desired tissue holds promises for future treatment of several diseases. Their nontoxic, biocompatible and safe nature are the key feature to make them site specific as well as long duration drug delivery carriers[57]. Their metal chelates are highly appropriate to use as magnetic resonance imaging contrast reagents[58].

**Polymeric micelles**

Polymeric micelles are nanoscopic copolymer micelle formed by lipophilic centre and the lipophobic block. The stability is achieved by corona of a lipophilic polymer chains. Polyethylene glycol (PEG) blocks form corona. Length of lipophilic centre forming block and that of hydrophilic block is similar[59]. Micelles forming surfactants improve solubility of a medicine with poor solubility in water besides increasing permeability of the medicine across physiological barriers and their bioavailability. Due to their smaller size and lipophilicity, polymeric micelles are retained for elongated duration in blood after intravenous delivery causing their reduced uptake by reticule- endothelial system. A target component when

attached to their surface is highly target specific. The medication is efficiently shielded from biological surroundings from possible deterioration due to their micellar nature[60]. Centre of lipophilic block of a polymeric micelle is stabilized by a corona of lipophilic polymeric chain. Due to micellar form, polymeric micelles find their path to the target organ or tissue.

**Polymeric nanoparticles**

Polymeric nanoparticles (PNP) although highly efficient and effective as intracellular delivery, site targeting systems and drug delivery as compared to conventional system, suffer from degradation, potential antigenicity and poor reproducibility. They may be in the form of nanocapsules (vesicular systems)[46] or nanospheres (matrix systems). The encapsulated drug release behaviour is controlled by manufacturing techniques. The drug may be dissolved, entrapped or encapsulated across or inside polymeric matrix. The drug is contained in the core enclosed by polymeric membrane while it is dispersed through the polymeric matrix. PNP have capability of customizing delivery of medicines and can be used as an excellent alternative in treatment of cancer[61]. Several efforts have been made to minimize the harmful effects of drugs during the delivery process to cure cancer and to prevent side effect on the nearby cells and tissues.

PNP can target the blood vessels which support tumour growth by supplying nutrients, oxygen etc., to cancer cells. They also target immune cells to develop anti-cancer immunotherapy[62].

**Solid lipid nanoparticles (SLN)**

SLN prepared from solid lipids stabilized by surfactants are used as a colloidal drug delivery system as a substitute to emulsions, liposomes and PNP. SLN show various advantages as drug delivery agent over other particle carriers besides targeted impact on brain[63,64,] such as better tolerance, biodegradability and high bioavailability and administration through eyes (ocular route). Small size SLN may be injected intravenously and could be used for site targeting of drugs[25].

**Nanoemulsions**

Nanoemulsions are made up of immiscible liquids, either oil in water type (o/w) into aqueous phase or vice versa. The oral bioavailability of isotropic mixture formed by mild mixing of oil, surfactant, co- surfactant and drug[65,66] (weakly water-soluble medicines) is improved by several processes. The small size of the droplets reduces the surface tension between the oil

droplets and aqueous medium of gastrointestinal tract permitting uniform drug distribution spread widely in the gut[67].

### Role of Nanotechnology in health care

NP with positive charge, small size and high surface to volume ratio can enter deep into the membranes and thus act as ideal vectors for gene delivery[68,69,70]. Some of the important nanoparticles utilised in gene therapy are liposomes, super paramagnetic iron oxide with fluorescent, quantum dot molecules

NP are relatively much better than viral vectors due to relative ease of preparation, almost nil risk of recombination and ability to load any size of gene.

Diseases like autoimmune disorders, viral infections and cancers may be treated by making the gene expression silent using small interferant RNA (siRNA). siRNA induces gene silencing through sequence specific cleavage of complementary messenger RNA molecule[71,72].

Gene could efficiently be delivered by conjugating gene materials such as RNA, DNA, siRNA with NP liposomes, polymeric and other nanomaterials. Genes are attached with NP by forming DNA-NP complex.

### Cardiovascular Diseases through NP

The treatment is carried out by introducing anti- apoptotic and pro-angiogenic genes into stem cells to improve rate of survival and their paracrine secretion[73,74]. Liposomes are one of the best NP for gene delivery as they do not permit non-specific binding of genes and avoid their degradation[75,76]. NP used should be highly target specific[77] and capable to track and monitor stem cells. Super paramagnetic iron oxide nano particles (SPION) are attached to cell surfaces and subjected to enter the cells. QD are also used for monitoring the living cells for long period. Growth factors have been delivered to placental cells using chitosan alginates NP to improve the functioning of cardiac tissues at the site of myocardial infarction[78].

### Treatment of brain diseases

Blood brain barrier (BBB), boundary between circulating blood and neural tissues of brain is the main obstacle in treatment of diseases related with brain as it prevents entry of the drug into central nervous system (CNS)[1]. Any sort of change in BBB causes neurodegeneration and neuro-inflammation and related diseases like Alzheimer (most common form of dementia) and Parkinson diseases (second most common form of brain disease) but the drugs are not allowed entry even after damage of BBB. However, due to their small size, high capacity of loading drugs and effective imaging performance (in case of inorganic NP) and

ability to conjugate with ligands, NP can cross BBB layer through several path ways and thus are capable of treating neurodegenerative diseases.

Some NP show therapeutic properties such as antioxidant, preventing beta-amyloid (Ab) peptide aggregation, decreasing reactive oxygen species (ROS) levels[79]. NP on conjugation with ligands interact to the optimum level with BBC receptors at low density through one of multiple pathways[69] so that it may cross BBB level and provide treatment of the related diseases such as Alzheimer's, Parkinson's etc. Circulation time of Zwitterion and neutral NP is greater in comparison to the charged NP[70,80].

**Application of nanotechnology for diagnosis and treatment of cancer**

Biocompatibility and time-consuming drug release characteristics of Nanoparticles made from PLGA polymer are utilised to load drug for cancer therapy. Anticancer drugs like doxorubicin, paclitaxel, 5- fluorouracil and dexamethasone prepared by utilising PLGA are highly effective for cancer treatment. Micro sphere version of Somatropin- PLGA Nanoparticle, Nutropin Depot, was authorized by food and drug administration (FDA) as anticancer drug, long back in 1999. The drug was approved as once per month to be administered as an alternative of human growth hormone (HGH) injection required daily to be taken[71]. Nanoparticles used in nano - oncology is highly effective to treat cancer due to its improved cancer cell targeting and overcomes cancer tissue multidrug resistance[72]. Doxorubicin primarily used to treat several types of cancer is highly toxic which effects heart and kidney also, besides tumour tissue but the same drug in liposomes is used as FDA approved nanomedical drug delivery system[81]. The liposomes formulation reduced doxorubicin passage to heart and kidney but enhanced doxorubicin accumulation[82].

**Nanoparticles in vaccination against Covid-19**

The recorded genome structure of SARS CoV-2 (corona virus) and knowledge of order of proteins laying the virus surface formed the basis for preparation of COVID-19 Nanoparticles based vaccines. The presence of spike proteins on the outer surface of the virus with a high connectivity towards nano-formulations and a high tendency to bind to host cell receptors was utilised as main point to develop CNPBV[83]. The FDA approved vaccine was highly effective in prophylaxis against COVID-19 to fight and restrict the spread of the Pandemic around the world. Pfizer-BioNTech and Moderna Vaccine were two vaccines relying on mRNA to encode the virus's spike glycoprotein (S) and incorporated the encapsulated modified mRNA into lipid base Nanoparticles[84] to aid transport of the protein antigen (spike protein) to immune cells and thus stimulating T cell activity induced antibody immunological response within the human body[85].

**Toxicity of NP**

Due to multiple applications of NP in medicines and other fields such as industrial etc., it becomes pertinent to have basic knowledge of toxic effects of NP to safeguard ourselves especially due to the fact that NP enters into the environment unnoticed due to its nanoscale size through air, water and soil by various activities of mankind.

Toxic effects of the NP being utilised for medical applications (CNT, QD, Iron oxide magnetic nanoparticles (IOMNP), liposomes and many others such as gold, silver, metal oxides, polymer NP) have been evaluated to a limited extent. In spite of toxicological effects being critical, there exists a wide gap between research on medical applications of NM and nano-toxicology[86]. Many of the NM useful in medicines show mild to almost nil toxicity.

However, studies reveal that even at very low aqueous concentration they effect environment in a significant way, for example, use of CdSe QD must be limited as they contain Cd which is reported to be toxic to cells at concentrations as low as $10 \, \mu gmL^{-1}$ [87].

CNT can enter into human cells and cause death of a cell by accumulating in cytoplasm[88]. The tubes have been observed to cause inflammation, fibrosis and toxicological effects in lungs[89] and may be easily inhaled due to its fibrous nature on dispersion in air and reach lungs. Among several studies made, AuNP of different shapes and sizes revealed almost negligible toxicity[90,91].

High reactivity, great capacity and small size of Magnetic NP making it advantageous could cause lethal effects by inducing adverse cellular toxic and harmful effects which is generally uncommon in micron sized counter parts. NP may translocate to different organs and tissues subsequent to entry into the body during ingestion or inhalation and cause toxicological effect. NP may aggregate in hard water or sea water and may be affected by some particular type of organic matter or colloids present in fresh water. Influence of Many abiotic factors for example pH, salinity, organic matter, state of dispersion of NP still remain to be ascertained responsible for NP to cause eco-toxicity[92]. AgNP is used as bandages, house hold items and even textiles due to its antimicrobial properties. Persistent exposure to silver may cause argyria and/ or argyrosis toxicity in human beings. High ratio of their surface area to volume in metal NP enhances release of Ag ions into solution but it's not confirmed that released silver from AgNP causes toxicity. Ag into solution causes toxic effects on aquatic species besides bacteria, algae, fish, and daphnia[92]. Interaction between Antigen and antibody labelled with fluorescent dyes, enzymes, radioactive materials or colloidal Au can help in detection of analytes in tissues which may help in assessment of toxicity[92].
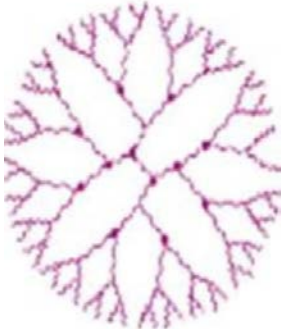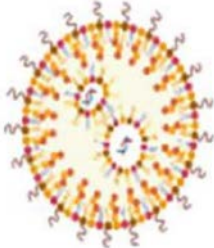
**Conclusion**
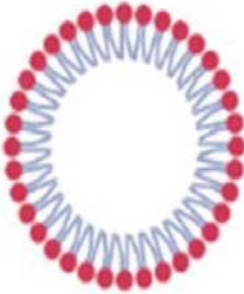
Nanotechnology is of immense use in drug related areas such as manufacturing and delivery of drugs besides their wide application in diagnostics. Nanoparticles have vital applications in medical field. Cancer diagnosis and treatment, gene therapy and genetic diseases like Alzheimer's, Parkinson's, Huntington's disease, amyotrophic lateral sclerosis, cystic fibrosis; nervous system disease, treatment of osteoporosis, broken bones, blood compatible heparin CNT as artificial kidney[28], vaccination against Covid-19; in implants, dentistry, MRI, DNA mutation[93] etc., are the various fields where nano particles play important roles. Table 1 lists detail of nanosystems (nanoparticles) and their applications. The prominent role of nanosystems (nanoparticles) in medicines is obviated by growing global market for them in the field expected to reach by 2027 to USD 182.3 billion at a compounded annual growth rate of 19.9% from 2021.

**Table:**

**Table 1**. Nanosystems/Nanoparticles utilised in Medicines

| Types of Nanosystems | Figures | Application | Problems and Solutions |
|---|---|---|---|
| Nanoparticles |  | Applied in therapeutics for treatment of cancer, stem cell diseases, implants and prosthetic orthopaedic diagnosis, in treatment of infectious and non-infectious diseases, production of vaccine, diagnosis of cancer employing bio imaging and immunisation, gene therapy, genetic disorders, brain and CNS (central nervous system) disorders, cardiovascular diseases, ocular diseases, delivery of drugs etc. | |

| | | | |
|---|---|---|---|
| Quantum Dots[31,32,33,34] |  | In diagnosis, in vivo bio imaging in real time, in controlling several diseases, in delivery of small interferent RNA for RNA interference, intracellular tracking and therapeutic drug delivery | |
| Dendrimers[56,57,58] |  | In diagnosis, gene delivery, as anticancer drugs, as antibacterial agent, in treatment of ocular diseases and as antigen carriers to modify vaccine formulations. | |
| Liposomes[46,48,49,50,51] |  | In hydrophobic and hydrophilic drug delivery, drugs protection from degradation by chemicals and enzymes, in capsulation of anti-tumour drugs such as dox, anthracyclines such epirubicin and daunorubicin etc. | |
| CNT (carbon nano tubes)[25,26,27,28, 93] |  | Drug delivery in delivering small organic drug molecules, peptides, proteins, nucleic acids into cells and controlled delivery of anticancer drugs, in treatment of broken bones Vaccine delivery, as vectors in gene delivery, heparin CNT as artificial kidney, biosensors, osteoporosis, early breast cancer detection, CNT x-ray for in-vivo imaging, in tumour therapy, DNA | Hurdles<br><br>Tendency to aggregate in large bundles and ropes especially in the media used commonly, (saline or serum) in toxicology.<br><br>Overcome by sonification, attaching of suitable functional group covalently |

| | | mutation [93] and disease protein biomarker detection | or making them stable by surfactant |
|---|---|---|---|
| Polymeric micelles[60] |  | In improving solubility of a medicine, permeability of the medicine across physiological barrier and their bioavailability, find their path to the target organ or tissue | |
| Polymeric nanoparticles (PNP)[61,62] |  | In intracellular delivery, site targeting system, in treatment of cancer, as target to immune cells to develop anticancer immunotherapy. | Drawbacks  Suffers from degradation, potential antigenicity, poor reproducibility |
| Niosomes[54, 55] | . | In delivery of potent drugs for treatment of cancer and viral diseases. | |
| Nanoemulsions[67] | | In uniform drug distribution in the gut | |

| | | | |
|---|---|---|---|
| Nanobubbles[38,39,41,43,44] | | To increase uptake of tumour cells on exposure to ultrasound, micro bubbles easily penetrate through brain blood barriers with a focused ultrasound, micro and Nanobubbles used for imaging and/or therapeutic use, MRI (magnetic resonance imaging with ultrasound therapy used in non-invasive thermal ablation method for cure of uterine fibroids, liver, bone prostrate and brain related diseases. | |
| Nanoshells[36] | | Used to cover specific shape particles to achieve desired morphology, gold nanoshells in enhancing targeting efficiency towards cancer cells. | |
| Paramagnetic Nanoparticles[45, 46] | | As effective target for specific organs under the effect of external magnet, super paramagnetic iron oxide with fluorescent in gene therapy, as contrast agents for MRI | |

**References**

1. S. Anjum, S. Ishaque, H. Fatima, W. Farooq, C. Hano, B. H. Abbasi and I. Anjum, Pharmaceuticals, 14, 707, 2021.
2. S. D. Jain, G. G. Sahastrbudhe and S. M. Pandey, Applied Physics, Universities Press, Hyderabad, 2012.
3. E. J. Chung, L. Leon and C. Rinaldi, Nanopartcles for Biomedical Applications: Fundamental Concepts, Biological Interactions and Clinical Application, Elsevier, Amsterdam, The Netherlands, 2019.

4. S. D. Li and L. Huang, Biochimica et Biophysica Acta Biomembranes, 1778(10), 2259, 2009.

5. A. N. Sahu, Int. J. Res. Ayurveda Pharm., 4, 472, 2013.

6. K. Subramani, W. Ahmed, Emerging Nanotechnologies in Dentistry, William Andrew: Norwich, NY, USA, 2017.

7. S. Laouini, A. Bouafia, M. Tedjani, Research Square, 2021. DOI: https// doi. org/10.21203/rs.3.rs-139856/ v1.

8. D. W. Hobson, In Intracellular delivery III, 405, 2016.[Cross Reference]

9. H. Agarwal, S. V. Kumar, S. Rajeshkumar, Resour. Effic. Technol., 3(4), 406, 2017.

10. K. Bogutska, Y. P. Sklyarov, Y. I. Prylutskyy, Ukr. Biorg. Acta, 1, 9, 2013.

11. A. U. Khan, M. Khan, M. H. Cho and M. M. Khan, Bioprocess Biosyst. Eng. 43, 1339, 2020.

12. A. Gagliardi, E. Giuliano, V. Eeda, M. Fresta, S. Bulotta, V. Awasthi and D. Cosco, Front. Pharmacol. 12, 601626, 2021. DOI: 10.3389/fphar.

13. H. Shiku, L. Wang, Y. Ikuta, T. Okugawa, M. Schmitt, X. Gu, K. Akiyoshi, J. Sunamato and H. Nakamura, Cancer Chemother Pharmacol., 46, S77, 2000.

14. J. M. Saul, A. V. Annapragda and R. V. Bellamkonda, J. Control. Release, 114, 277, 2006.

15. R. P. Prajnamitra, H. -C. Chen, C. J. Lin, L. L. Chen and P. C. -H Hsieh, Molecules, 24(10), 2017, 2019.

16. G. Amoabediny, F. Haghiralsadar, S. Naderinezhad, M. N. Helder, E. K. Akhoundi, J. A Mohammadnejad and B.D. Zandieh, Int. J. Polymfor . Mater polym Biomater, 67(6), 383, 2018

17. D. R. Wilson, R. Sen, J. C. Sunshine, D. M. Pardoll, J. J. Green and Y. J. Kim, Nanomed Nanotechnol. Biol Med., 14(2), 237, 2018.

18. D. S. Kohane, Biotechnol. Bioeng., 96(2), 203, 2007.

19. J. Panyam and V. Labhasetwar, Adv. Drug. Deliv. Rev. 55(3), 329, 2003.

20. S. A. Rizvi and A. M. Saleh, Saudi Pharm J., 26(1), 64, 2018.

21. V. Mohanraj and Y. Chen, Trop. J. Pharm. Res., 5(1), 561, 2006.

22. J. Zhang and M. Saltzman, Chem. Eng. prog., 109 (3), 25, 2013.

23. T. N. Vo, F. K. Kasper and A. G. Mikos, Adv. Drug.Deliv. Rev., 64(12), 1292, 2012.

24. R. M. Riely, J. Nucl. Med., 48(7), 1039, 2007.

25. M. Benincasa, S. Pacor, W. Wu, M. Prato, A. Bianco and R. Gennaro, American Chemical Society, Nano 5(1), 199, 2011.

26. Z. H. Saad, R. Jahan and U. Bagul, Asian J Biomed Pharm Sci, 14, 11, 2012.

27. P. Dey and N. Das, Int. J. Pharm. Pharm Sci, 5, 9, 2013.

28. A. Eftekhari, S. M. Dizaj, E. Ahmedian, A. Prezkora, S. M. H. Khatibi, M. Ardalan, S. Z. Vahed, M. Valiyeva, S. Mehraliyeva, R. Khalilov, M. Hasanzadeh, Materials (Basel), 14(11), 2039, 2021.

29. E. J. Chung, L. Leon and C. Rinaldi, Nanoparticles for Biomedical Applications: Fundamental Concepts, Biological Interactions and Clinical Application, Elsevier, Amsterdam, The Netherlands, 2019.

30. I. Medintz, A. Clapp, H. Mattousi, E. Goldman, B. Fisher, J. Mauro, Nat. Mater., 2, 630, 2003.

31. M. Bruchez jr., M. Moronne, P. Gin, S. Weiss, A. P. Alivisatos, Science, 281, 2016, 1998.

32. A.M. Iga, J. H. Robertson, M.C. Winslet and A. M. Seifalian, Bio Med Res Int, 10,76087,2007.

33. M. Schwarczynski and I. Toh, Micro-and Nanotechnology in Vaccine Development, Wulliam Andrew, Norwich, NY, USA, 2016.

34. R. E. Bailey, A. M. Smith and S. Nie, Phys E, 25(1), 1, 2004.

35. S. W. Kalale, S. Gosavi, J. Urban and S. Kulkarni, Current Science, 91(8), 1038, 2006.

36. C. Loo, A. Lowery, N. Halas, J. West and R. Drezek, Nano Lett., 5(4), 709, 2005.

37. J. N/ Meegoda, S.A. Hewage and J. H. Batagoda, http://doi/10.1089/ees.2018.0203.

38. Z. Gao, A. M. Kennedy, D. A. Christensen, N. Y**. Rapoport, Ultrasonics, 48(4), 260, 2008.

39. A. L. Klibanov, Investig Radiol, 41(3), 354, 2006.

40. C. Zhang, Y. Li, X. Ma, W. He, C. Lin and Z. Liu, Scince China Chemistry, 64(6), 899, 2021

41. Y. Li, Drug Efflux Pumps in Cancer Resistance Pathways, from Molecular Recognition and Characterization to Possible Inhibition Strategy in Chemotherapy, Science China Press and Springer- Vertlag GMBH Germany (part of Springer Nature),2021.

42. J.S. Xu, J. Huang, R. Quin, G. H. Hinkle, S. p. Povoski, E. W. Martin, R. X. Xu, Biomaterials, 31, 1716, 2010

43. S. R. Scgreglmann, R. Bauer, S. Hagele - Link, K. P. Bhatia, P. Natchev, N. Wegener, A. Lebeda, B. Werner, E. Martin, G. Kagi, Neurology, 88, 1329, 2017.

44. F. A. Jolesz, Annu. Rev. Med., 60, 417, 2009.

45. A. G. Cuenca, H. Jiang, S. N. Hochwald, M. Delano, W. G. Cance, S. R. Grobmyer, Cancer, 107(3), 459, 2006.

46. Z. M. Mazayen, A. M. Ghoneim, R. S. Elbatanony, E. B. Basalious and E. R. Bendas, Future Journal of Pharmaceutical Science, 8, 12, 2022.

47. V. P. Torchilin, Nat. Rev. Drug Discov., 4(2), 145, 2005.

48. P. Laverman, M. G. Carstens, O. C. Borrman, E. T. Dams, W. J. Oyen, N. Van Rooijen, F. H. Corstens, G. Storm, J. Pharmacol Exp Ther, 298(2), 607, 2001.

49. V. Nekkanti, S. Kalepu, Pharm Nanotechnol, 3(1), 35, 2015.

50. A. A. Gabizon, H. Smeeda, S. Zalpsky, J Liposome Res, 16(3),175, 2006.

51. K. Cho, X. Wang, S. Nie, Z. G. Chen, D. M. Shin, Clin Cancer Res, 14(5), 1310, 2008.

52. S. Moghassemi, A. Hadjizadeh, J Control Release, 185, 22, 2014.

53. K. M. Kazi, A. S. Mandal, N. Biswas, A. Guha, S. Chatterji, M. Behera, K. Kuotsu, J Adv Pharm Technol Res, 1(4), 374, 2010.

54. T. Malik, G. Chauhan, G. Rath, R. N. Kesarkar, A. S. Chowdhary, A. K. Goyal, Artif Cells Nanomed Biotechnol, 46(sup 1), 79, 2018.

55. H. S. Shah, F. Khalid, S. Basir, M. H. Bin Asad, K. U. Rehman Khan, F. Usman, I. Javed, J Nanopart Res, 21(2), 1, 2019

56. S. M. Moghimi, A. C. Hunter, J. C. Murray, FASEB J, 19(3), 311, 2005.

57. M. Keshand, B. Goswami, Int, J. Pharm. And Biosci., 9(1), 681, 2019.

58. H. N. Patel and P. M. Patel, Int. J. Pharm. Biosci., 4(2), 454, 2013.

59. V. Torchilin, Cell Mol Life Sci CMLS, 61(19-20), 2549, 2004.

60. S. Sahoo, S. R. Mishra, S. Parveen, Nanomedicine, 8(2), 147, 2017.

61. O. Kayser, A. Lemke, N. T. Hernandez, Curr Pharm Biotechnol, 6(1), 3, 2005.

62. J. Karlsson, H. J. Vaughan and J. J. Green, Annu Rev Chem Biomol Eng., 9, 105, 2018.

63. R. Cavalli, M. R. Gasco, P. Chetoni, S. Burglassi, M. F. Saettone, Int J pharm, 238(1-2), 241, 2002.

64. S. C. Yang, L. F. LuY. Cal, J. B. Zhu, B. W. Liang, C.Z. Yang, J Control Release, 59(3), 299, 1999.
65. K. K. Singh, S. K. Vingkar, Int J Pharm, 347(1-2), 136, 2008.
66. S. Nazzal, II Smalyukh, O. D. Laverntovich, M. A. Khan, Int J Pharm, 235(1-2), 247, 2002.
67. Z. Cal, Y. Wang, LJ Zhu, Z. Q. L iu, 11(2), 197, 2010.
68. C. Saraiva, C. Praca, R. Ferreira, T. Santos, L. Ferreira and L. Bernardino, J. Control. Release, 235,34,2016.
69. S. M. Lombardo, M. Schneider, A. E. Tureli and N. G. Tureli, J. Nanotechnol., 11, 866, 2020. [CrossRef]
70. M. Pautler and S. Brenner, Intl.J. Nanomed., 5, 803, 2010.
71. S. Acharya and S. K. Sahoo,Adv. Drug Delivery, 63(3), 170, 2011.
72. N. H. Goradel, F. H. Ghiyami, S. Jahagiri, B. Negahiari, A. Sahebkar, A. Masoudifar and H. Mirzaei, J Cell Physiol 233(4),2902, 2018.
73. T. Deuse, C. Peter, P. W. Fedak, T. Doyel, H. Reichenspurner, W. H. Zimmermann, T. Eschenhagen, W. Stein, J. C. Wu, R. C. Robbins, Circulation, 120, S247, 2009. [CrossRef][PubMed]
74. J. Tang, J. Wang, J. Yang, X. Kong, F. Zheng, L. Guo, L. Zhang and Y. Huang, Eur. J. Cardio Thorac. Surg., 36, 644, 2009. [CrossRef][PubMed]
75. D. Pack, A. Hoffman, S. Pun and P. S. Stayton, Nat. Rev. Drug. Discov., 4,581, 2005.
76. L. Zhang, F. Gu, J. Chan, A. Wang, R. Lanjer and F. Farokhzad, Therapeutics 83, 761, 2008.
77. Z.-K. Cui, J. Fan, S. Kim, O. Bezouglaia, A. Fartash, B. M. Wu, T. Aghaloo and M. Lee, J. Cotrol. Release, 217, 42, 2015. [CrossRef][PubMed]
78. Z. M. Binsalamah, A. Paul, A. A. Khan, S. Prakash and D. Shum-Tim, Int. J. Nanomed., 6, 2667, 2011.
79. X. Niu, J. Chen and J. Gao, Asian J. Pharm. Sci. 14, 480, 2019.
80. C. H. J. Choi, C. A. Alabi, P. Webster and M. E. Davis, Proc. Natl. Acad. Sci. USA, 107,1235, 2010.
81. S. A. Abraham, D. N. Waterhouse, L. D. Mayer, P. R. Cullis, T. D. Madden and M. B. Bally, Methods Enzymol, 391, 71, 2005.
82. T. Safra, F. Muggia, S. Jeffers, D. D. Taso-Well, S. Groshen, O. Lyass, R. Henderson, G. Berry and A. Gabizon, Ann Oncol, 11(8), 1029, 2000.
83. M. D. Shin, S. Shukla, Y. H. Chung, V. Beiss, S. K. Chan, O. Rivera-Ortega, D. M. Wirth, A. Chen, M. Sac, J. K. Pokorski and N. F. Steinmetz, Nat Nanotechnol, 15(8), 646, 2020.
84. R. Noor, Curr Clin Microbiol Rep, 3, 1, 2021.
85. T. M. Belete, Infect Drug Resist, 14, 151, 2021.
86. Z. P. Aguliar, Nanomaterials for Medical Appreciations, Chapter9, P 363, Elsevier, USA, 2013.
87. J. Lovric, H. S. Bazzi, Y. Cuie, G. R. Fortin, F. M. Winnik and D. Maysinger, J. Mol. Med. 83, 377, 2005.
88. A. Porter, M. Gass, K. Muller, J. Skepper, P. A. Midgley and M. Welland, Nat. Nanotech., 2, 713, 2007.

89. R. Zumw alde and L. Hodson, Approaches to Safe Nanotechnology: Managing the Health and Safety Cocerns, Associated with Engineered Nanomaterials, DHHS (NIOSH), Publication No. 2009-125, 2009.

90. A. C. Subuncu, J. Grubbs, S. Quian, T. M. Abdell- Fattah, W. M. Stacey and A. Beskok, Colloids Surf. B, 95, 96, 2012.

91. J. E. Gagner, M. D. Lopez, J. S. Dordick and R. W. Siegel, Biomaterials, 32, 7241, 2011.

92. I. Khan, K. Saeed, I. Khan, Arabian Journal of Chemistry, 12, 908, 2019.

93. S. Modi, R. Prajapati, G. K. Inwati, N. Deepa, V. Tirth, V. K. Yadav, K. K. Yadav, S. Islam, P. Gupta, D. H. Kim and B. H. Jeon, Crystal, 12, 39, 2022.

# A Minireview on The Applications of Nanobiosensors Based on Localized Surface Plasmon Resonance

Chandrashekhar P. Pandhurnekar*[1], Himani C. Pandhurnekar[2] and Avinash V. Bharati[1]

1*. Department of Chemistry, Shri Ramdeobaba College of Engineering and Management, Nagpur, Maharashtra, India 440 013.
2. Department of Chemistry, Dada Ramchand Bakhru Sindhu Mahavidyalaya, Nagpur, Maharashtra, India 440 017.
* Email: pandhurnekarcp@rknec.edu

**Abstract:**

In this new era of nano-materials, most chemists and physicists are familiar with the phenomenon of localized surface plasmon resonance (SPR). Noble-metal nano-particles with dimensions (3–100 nm) much smaller than the wavelength of incident light (400–900 nm) exhibit this tendency. In nanostructured materials, due to their very small particle size, the electrons are restricted within the nanoparticle surface area and oscillate with a certain frequency. It is noteworthy that the phenomenon of localized surface plasmon resonance appears when the frequency of the incoming photons overlaps with the frequency of the electrons. As this oscillation of surface electrons is taking place against the restoring forces of the positive nuclei, there is a formation of plasmon resonance. This characteristic property of scattering and absorption of photons appearing in the SPR of every nano-structured material, make them excellent nanoprobes for a variety of applications such as cell imaging and detection of protein phosphorylation and many others. The performance of bio-chemical sensing devices has been greatly improved by the development of localized surface plasmon resonance (SPR) based sensors. In the present minireview, we have briefly discussed the classification of biosensors and the basics of their instrumentation.  Some of these applications have been discussed here using some nano-engineered biosensors.

**Key words:** Surface plasmon resonance, Sensors, Nanomaterials, Nanotechnology, Biosensors.

**Introduction:**

An optical sensor is a piece of detecting equipment that, through the use of light, transforms the quantity under-measure into another variable, which is often recorded into one of a light wave's properties. At the interface of a metal film and a dielectric material (superstrate), in which alterations in refractive index are to be detected, a surface plasmon is excited in SPR sensors. The surface plasmon's propagation constant changes when the superstrate's refractive index changes. An alteration in one of the properties of the optical wave interacting with the surface plasmon can be seen as a result of this modification, which modifies the linking situation between a light wave and the surface plasmon. A potent tool for the label-free, authentic surveillance of biological molecules is the surface plasmon resonance (SPR) based sensing technique. In SPR-based biosensors, targeted molecules selectively receptors located on the sensor surface, causing changes in the sensor's refractive indices that may be monitored for label-free, real-time identification of a variety of target analytes.

Bionanomaterials are widely studied in the last 10 years. To increase applications in medical fields, novel structure and functionalities are the key factors.[1–8] Important nanomaterials used are nanofibers, nanotubes and nanowires, etc.[9–16] Optical nanosensors are new development which is suitable for intracellular applications. Their applications in the monitoring of in-vivo biological processes could greatly improve current knowledge of cellular functions. Optic nanosensors could be chemical sensors and biosensors.[17-19] Amongst all these biosensors are the most widely used. Many works are also done on gold biosensors,[20-23] titanium biosensors,[24] quantum dots biosensors,[25-29] and carbon nanotube biosensors.[30] Many nano-enabled medical products have already hit the market, and the industry is likely to boom in the next years as applications extend and pervade more complex diseases including cancer, cardiac and neurological disorders, infection, tissue engineering, and many more.

The concentration of a certain analyte or collection of analytes is related to a measured response by bio-sensors, which are analytical devices that combine a biological recognition component with a signal transducer. The kind of transducer and/or recognition molecule that biosensors use is commonly categorised. The majority of biosensors recognise and bind a

molecule of interest before catalysing a chemical conversion of that molecule into a product that is subsequently detected, such as antibodies, nucleic acids, and hormone receptors, as well as enzymes and microbial cells. By transforming the biological reaction into usable electrical signals, the transducer may detect any interactions between the affinity-pairing partners. After being transformed, the electrical signal is evaluated by a processor. The basic configuration of a biosensor is illustrated in Fig. 1.[31]

Nanoparticles, nanowires (NWs), and nanotubes (NTs) have all been widely explored and exploited in innovative biosensor devices thanks to recent advancements in fabrication processes.[32]

**Classification of biosensors:**

Bio-sensors can be broadly classified as (a) Direct label-free detection biosensors and (b) Indirect label-based detection biosensors. Direct label-free detection biosensors are built on biochemical interaction principles discovered through real-time analysis. Non-catalytic ligands, such as cell receptors or antibodies, are used in this approach. During these interactions, these biosensors may detect minute changes in optical, mechanical, and electrical properties, as well as any tagged moieties. Localised surface plasmon resonance sensors are a common type of ephemeral biosensor. Interferometric and grating sensors are two other types of detecting sensors. Indirect label-based detection biosensors, on the other hand, rely on auxiliary elements for identification and use labelled or catalytic elements like enzymes. Alkaline phosphatase enzymes and fluorescently labelled antibodies are examples of auxiliary elements. This approach, unlike direct label-free detection biosensors, necessitates the connection of the tagged species to the detecting site. The majority of optical indirect sensors are based on the principles to detect fluorescence, although they can also be monitored for densitometric, colorimetric, and chemiluminescence changes depending on the label employed.

Newer technology such as nanomaterials, artificial intelligence-based integrated optics (IO), graphene bioelectronics, AI-based medical portable imaging, novel fluidics and fabrication methodologies, and new cellular and molecular approaches are currently being applied in biosensors.[33]

**Surface Plasmon Resonance (SPR) Biosensors Instrumentation:**

An optical system, supporting electronics, and a technique for gathering and processing sensor data make up an SPR sensor instrument. In the optical system, surface plasmons are produced optically. The resulting light wave is recognised and examined to gather the required information. It carries an SPR signal that is encoded. The detector signal is processed to produce the sensor output. Along with sample handling and preparation procedures, a bio-recognition coating on SPR biosensors interacts with target molecules in a liquid sample. Even the slightest changes in the refractive index can be detected using the non-destructive optical technique known as SPR. Figure 2 depicts its components: a light source, prism, gold film, and detector.[34]

A light pulse activates surface plasmons in an SPR sensor's optical system. In the SPR sensor, surface plasmon stimulation causes a change in one of the light wave's characteristics. SPR sensors are categorised as (i) angular, (ii) wavelength, (iii) intensity, (iv) phase, or (v) polarisation modulated, depending on which property of the light wave is modified and employed as a sensor output. In today's SPR sensors, the first three types of modulation are most commonly utilized.[35]

**SPR sensors based on prism couplers and wavelength modulation:**

Based on wavelength modulation, Homola et al. [35] developed a functioning modular SPR sensor. The sensor consisted of a halogen lamp, SPR sensor platform, and spectrometer. White light was sent from the halogen lamp to the SPR sensor platform through a multimode optical link. A large diameter parallel beam input collimator, polarizer, and multichannel output collimator, as well as a glass prism with an attached SPR chip, were all part of the sensor platform (coated in a 50 nm thick gold coating). The output collimators, which were coupled to the spectrograph's inputs, connected the light into optical fibres.[35] By checking for a change in reflectivity in the linear region of the SPR angular or spectral response curve, one can detect the shift of the SPR dip in the intensity interrogation mode. The variation in the refractive index is inversely correlated with the variation in the SPR signal in the linear region above the metallic sheet. This necessitates changing and fine-tuning the incidence angle and wavelength of the excitation light for maximum sensitivity. An example of a prism-based intensity interrogation SPRi setup is shown in Fig. 3. On the sensor surface, the

charge-coupled device (CCD) camera continuously records a sequence of 2D intensity contrast images.[36]

**Advancements in the localized surface plasmon resonance (lspr) biosensors technology:**

Surface plasmon resonance at the microscale and localised surface plasmon resonance at the nanoscale sensing have proven to be very powerful next-generation probing technologies in the current Covid-19 outbreak. The maximum absorption wavelength deviation can be used by the LSPR. This is due to an increase in the intensity of fluorescent light created by near-field light, as well as a change in the local index of refraction on the surface of the Nano-material probe used as a sensing device.

The fibre optic surface plasmon resonance (SPR) sensor system for cellphones, seen in Fig. 4, was first published by K. Bremer *et al.* [37] A simple silver coating procedure was used to create the sensor, and both ends of a 400 m optical fibre were polished to create 45° end-faces. The smartphone's backside flashlight and camera were used, respectively, for activating and querying the SPR sensor system. Consequently, the created sensor system does not need any external electrical components to function. A refractive index sensor was created as an initial use case. Different volume concentrations of glycerol solution were used to show how well the SPR sensor system performed.

SPR biosensors have recently drawn a lot of interest as medical diagnostic tools for a variety of reasons. They can be quickly and cheaply prepared without labels. A reusable magnetic surface plasmon resonance (SPR) sensor chip was created by Yoo et al. to repeatedly detect different target molecules in a typical SPR system. We showed that it is possible to measure the nucleoprotein (NP) of the H1N1 influenza virus solution repeatedly more than 7 times with a single reused SPR sensor chip without noticeably degrading the signal. Additionally, a single SPR chip might be used to repeatedly measure various target molecules. The cost of SPR sensing should be greatly decreased because our reusable SPR sensor chip can be used repeatedly in a traditional SPR system without the need for chemical treatments for refreshment.[38]

Differential levels of microRNA expression are found in cancer, and they have an impact on metastasis, carcinogenesis, and cellular transformation. Although dye molecule labels for

fluorescence approaches have been investigated, label-free molecular-level measurement of miRNA is incredibly difficult. For the precise label-free detection of therapeutically important biomarkers like miRNA-21 and miRNA-155, Tianyu Xue and colleagues developed a surface plasmon resonance sensor based on two-dimensional antimonene nanomaterial. Since antimonene contains more delocalized 5s/5p orbitals than graphene, which has previously been employed in DNA molecule sensing, first-principles energetic calculations show that antimonene has a significantly stronger interaction with ssDNA. The detection threshold can be raised to 10 aM, which is 2.3–10,000 times greater than that of current miRNA sensors.[39]

For an early ovarian cancer diagnosis, the discovery of the biomarker human epididymis secretory protein 4 (HE4) is essential. Y. Jialing, *et al.*[40] sought to develop a novel localised surface plasmon resonance (LSPR) biosensor for detecting HE4 using blood samples from ovarian cancer patients. The conceptual design of this biosensor is as shown in Fig. 5 and Fig. 6.[40] In experiments for the detection of HE4, the LSPR-based biosensor was discovered to have a quick detection speed, strong specificity, effective repeatability, and long-term stability. The linear range for LSPR was between 10 and 10,000 pM with a detection limit of 4 pM. The results of the enzyme-linked immunosorbent test and the LSPR have a very strong correlation in human serum. Patients with ovarian cancer were shown to have human epididymis secretory protein 4 in their serum using a label-free LSPR technique.[40]

**The Summary, Future Perspectives, and Challenges:**

Review of the development trend for SPR sensors based on light source technology. One of the most demanding applications for the SPR sensor's ultralow detection limit is in the realm of medicine, where early biomarker identification is one of the most common uses. Nanoelectronics manufacturing and technology are advancing quickly to reach smaller devices. The development of smartphone-based SPR sensors has amazingly served as a crucial turning point in the merging of digital technology with biosensor application technologies and lab-on-chip platforms. Internet-of-things (IoT) technology will indefinitely play a significant role in the data transmission of the SPR sensor in clinical settings.

The main challenges to the study and development of SPR sensors are the expensive platforms and components. Commercial platforms often do not cover the expense requirements of small research groups or points of care (PoC) to invest in and maintain. As a

result, it offers a feasible route for scientists and engineers working in both the academic and industrial sectors to develop a low-cost yet powerful SPR sensor platform in the future.[41]

**Conclusions:**

When nanomaterials or nanostructures are utilised in biosensors, their unique physicochemical properties open up a whole new world of sensing options. As a result, nano-bio-sensing is an excellent illustration of how material sciences, physics, chemistry, and biology interact at the nanoscale. Nanomaterials and nanostructures have unique physicochemical properties that cannot be obtained by normal bulk materials, which bodes well for the future of this field.

The most recent sample publications looked at the claim that combining biomolecules with nanomaterials and nanostructures can result in biosensors with improved sensitivity and selectivity, faster reaction times, decreased power consumption, and feasible miniaturisation.[42] Real-time and label-free SPR-based biosensors are widely used by the pharmaceutical industry and fundamental researchers. Biosensors can be used for a plethora of different things, from qualitative binding to high-resolution kinetic analysis. Almost every interaction involving biological systems can be studied using these methods, including those involving proteins, nucleic acids, and even lipid surface environments. SPR-based technology will unavoidably advance as platforms with greater throughput and sensitivity are created in the future.

**Figures:**
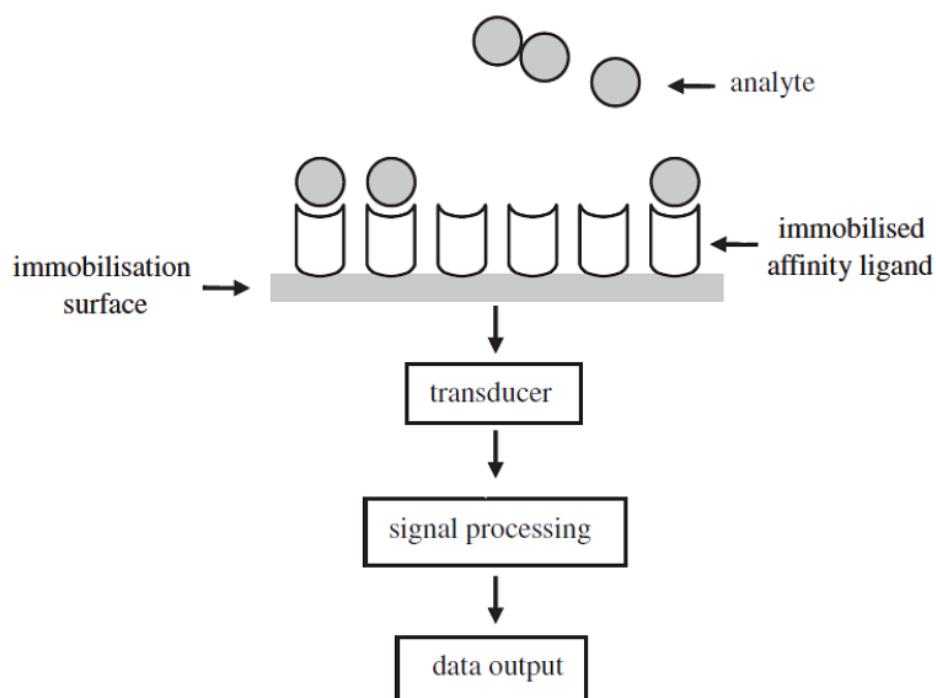


**Fig. 1:** General schematic of biosensors. Adapted from Mungroo, *et al.*[31]
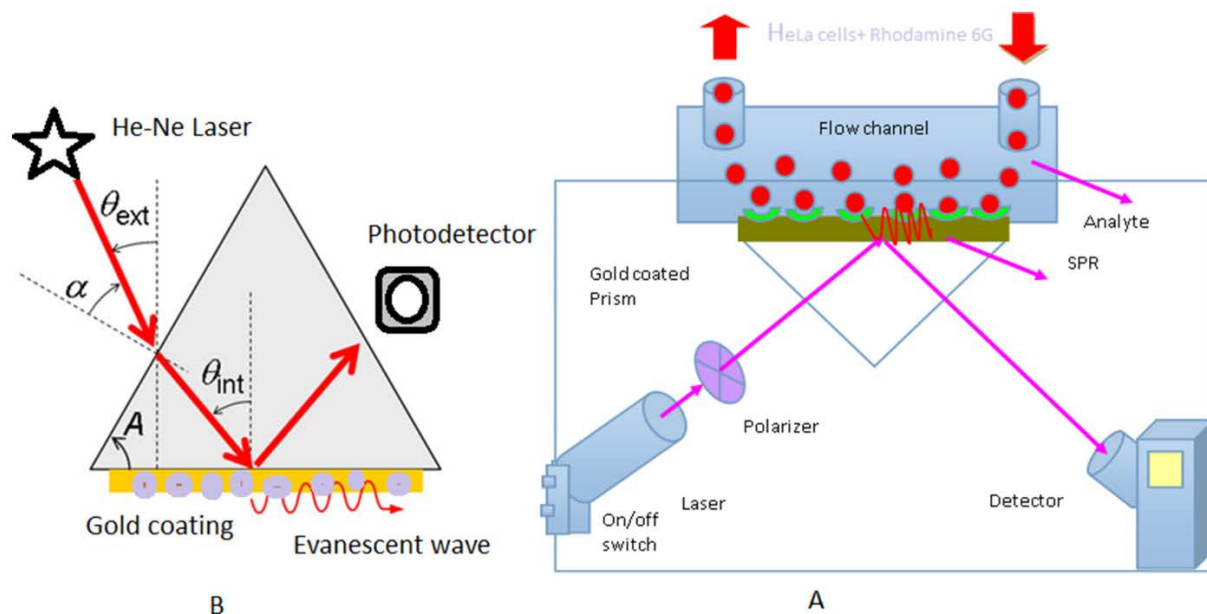
**Fig. 2:** Schematic of an SPR (bio)sensors. Adapted from Firdous, *et al.*[34]
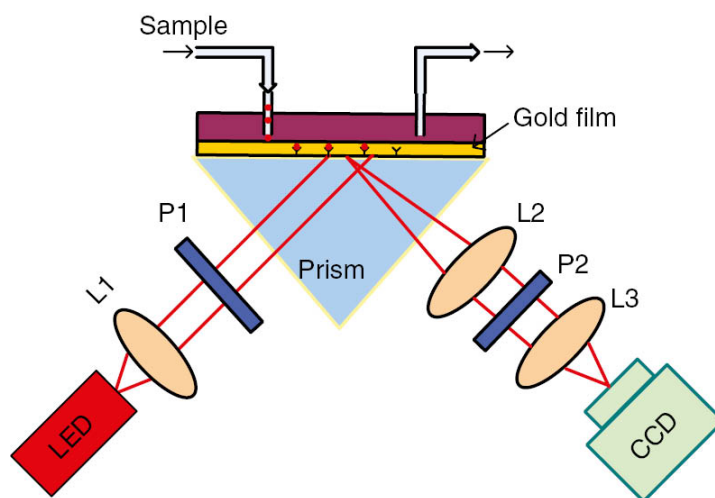


**Fig. 3:** Schematic illustration of a typical prism-based intensity interrogation SPRi setup. Adapted from Zeng, *et al.*[36]
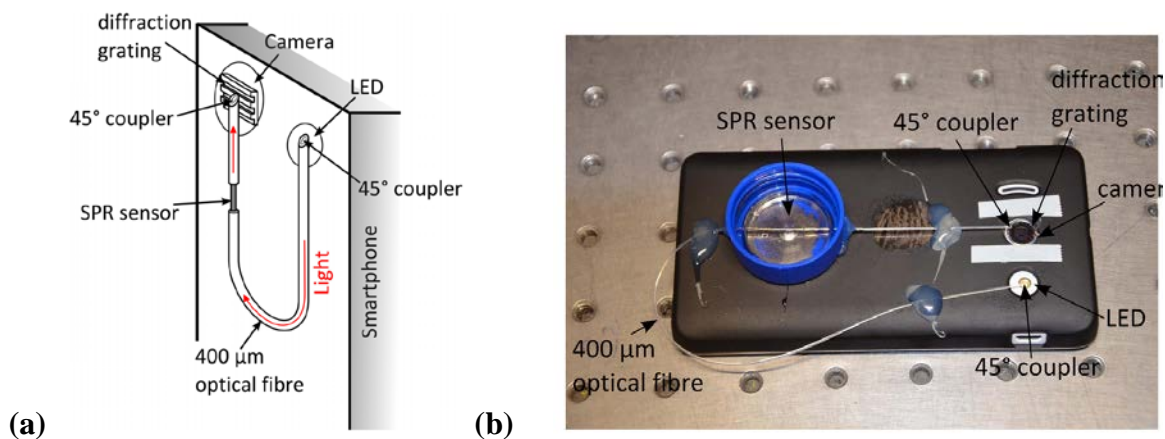
**Fig. 4: (a)** Schematic of the fibre optic SPR sensor system for Smartphones **(b)** Picture of the fibre optic SPR sensor system. Adapted from K. Bremer *et al.* [37]
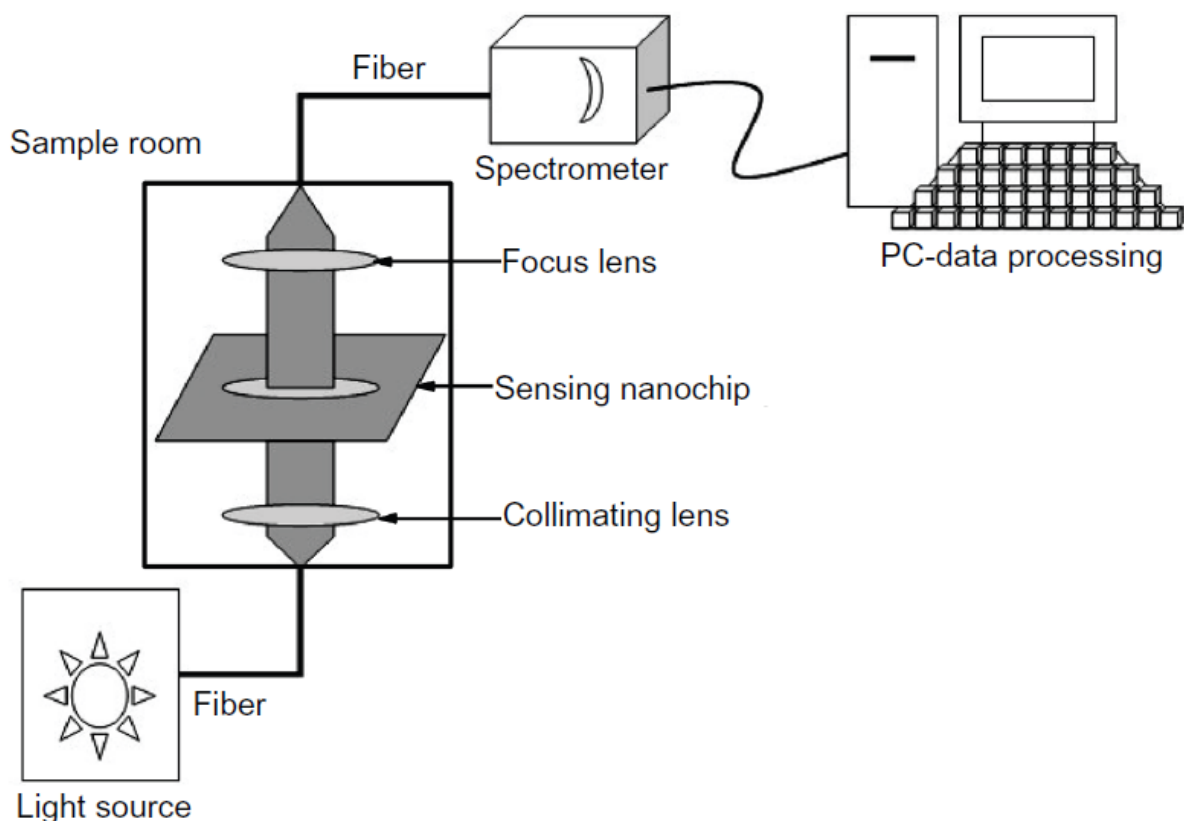


**Fig. 5:** Schematic representation of experimental set up of localized surface plasmon responance biosensor. Adapted from Y. Jialing, *et al.* [40]
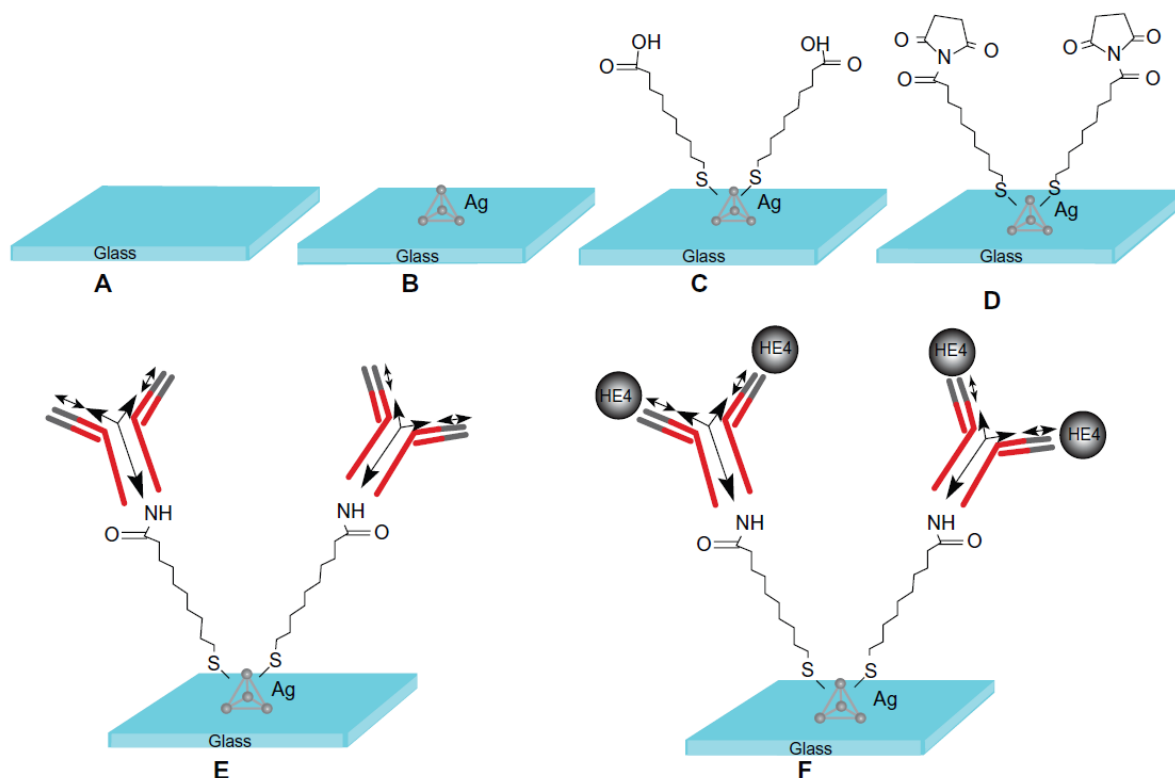
**Fig. 6:** Design of the localized surface plasmon resonance biosensor for HE4 detection using a direct assay format. (**A**) Glass substrate, (**B**) silver nanoparticles synthesized through NSL technology, (**C**) A self-assembled monolayer layer formed by incubation in 1 mM 11-mercaptoundecanoic acid, (**D**) incubation in 75 mM 1-ethyl-3-(3-dimethylaminopropyl) carbodiimide hydrochloride/15 mM N-hydroxysuccinimide, (**E**) anti-HE4 antibody (10 µg/mL) covalently attached to the nanoparticles, and (**F**) different concentrations of the HE4 both in buffer and serum samples reacted with the anti-HE4. **Abbreviation:** HE4, human epididymis secretory protein 4. Adapted from Y. Jialing, *et al.* [40]

**References:**

1. T. Tarhan, A. Dündar, V. Okumuş and M. Çulha, Chemistry Select, 6 (17), 4217, 2021.

2. A. Agi, R. Junin, M. Z. Jaafar, M. A. Sidek, F. Yakasai, A. Gbadamosi and J. Oseh, J. Ind. Eng. Chem., 98, 82, 2021.

3. M. M. H. Chowdhury, C. J. J. Salazar and M. Nurunnabi, Biomater. Sci., 9 (14), 4821, 2021.

4. B. Prickril and A. Rasooly, Biosensors and Biodetection - Methods and Protocol, Volume 2: Electrochemical, Bioelectronic, Piezoelectric, Cellular and Molecular Biosensors, Humana Press, New York, 2017.

5. N. Ashraf, S. H. Sumrra, M. A. Assiri, M. Usman, R. Hussain, F. Aziz, A. Hussain, M. A. Ghaffari, M. N. Qaisar, M. Imran and A. Irfan, Green Process. Synth., 10 (1), 476, 2021.

6. S. Aleksei and U. Shimanovich, Isr. J. Chem., 60(12), 1152, 2020.

7. E. Stone, V. Pennone, K. Reilly, I. R. Grant, K. Campbell, E. Altermann and O. McAuliffe, Foods, 11(6), 854, 2022.

8. P. Lyu, P. Javidi-Parsijani, A. Atala and B. Lu, Nucleic Acids Res., 47 (17), e99, 2019.

9. Y. Chen, Z. Lai, X. Zhang, Z. Fan, Q. He, C. Tan and H. Zhang, Nat. Rev. Chem., 4(5), 243, 2020.

10. H. Xu, H. Shang, C. Wang and Y. Du, Adv. Funct. Mater., 30(50), 2006317, 2020.

11. N. Baig, I. Kammakakam and W. Falath, Mater. Adv., 2(6), 1821, 2021.

12. S. Priyadarsini, S. Mohanty, S. Mukherjee, S. Basu and M. Mishra, M., J. Nanostructure Chem., 8 (2), 123, 2018.

13. S. J. Choi and I. D. Kim, Electron. Mater. Lett., 14 (3), 221, 2018.

14. S. Nasir, M. Z. Hussein, Z. Zainal and N. A. Yusof, Materials, 11(2), 295, 2018.

15. Y. H. Teow and A. W. Mohammad, Desalination, 451, 2, 2019.

16. Y. Zhu, L. Peng, Z. Fang, C. Yan, X. Zhang and G. Yu, Adv. Mater., 30(15), 1706347, 2018.

17. Y. Sun, L. Shi, L. Mi, R. Guo and T. Li, J. Mater. Chem. B, 8(24), 5178, 2020.

18. P. Sharma, V. Pandey, M. M. M. Sharma, A. Patra, B. Singh, S. Mehta and A. Husen, Nanoscale Res. Lett., 16(1), 1, 2021.

19. M. Javaid, A. Haleem, R. P. Singh, S. Rab and R. Suman, Sensors International, 2, 100130, 2021.

20. M. K. Masud, J. Na, T. E. Lin, V. Malgras, A. Preet, A. A. I. Sina, K. Wood, M. Billah, J. Kim, J. You and K. Kani, Biosens. Bioelectron., 168, 112429, 2020.

21. S. Han, W. Liu, M. Zheng and R. Wang, Anal. Chem., 92(7), 4780, 2020.

22. B. Negahdari, M. Darvishi and A. A. Saeedi, Artif. Cells Nanomed. Biotechnol., 47(1), 455, 2019.

23. V. B. Borse, A. N. Konwar, R. D. Jayant and P. O. Patil, Drug Deliv. Transl. Res., 10(4), 878, 2020.

24. N. P. Shetti, S. D. Bukkitgar, K. R. Reddy, C. V. Reddy and T. M. Aminabhavi, Colloids Surf. B: Biointerfaces, 178, 385, 2019.

25. C. Ji, Y. Zhou, R. M. Leblanc and Z. Peng, ACS sensors, 5(9), 2724, 2020.

26. S. Campuzano, P. Yáñez-Sedeño and J. M. Pingarrón, Nanomater., 9 (4), 634, 2019.

27. R. R. Pandey, and C. C. Chusuei, Molecules, 26(21), 6674, 2021.

28. W. Jiang, Y. Zhao, X. Zhu, H. Liu and B. Sun, Adv. NanoBiomed Res., 1(6), 2000042, 2021.

29. Z. Hassanvand, F. Jalali, M. Nazari, F. Parnianchi and C. Santoro, ChemElectroChem., 8(1), 15, 2021.

30. M. Sireesha, V. Jagadeesh Babu, A. S. Kranthi Kiran, and S. Ramakrishna, Nanocomposites, 4(2), 36, 2018.

31. N. A. Mungroo, S. Neethirajan, Biosensors, 4, 472, 2014.

32. V. Buk and M. E. Pemble, Electrochim. Acta, 298, 97, 2019.

33. A. Banerjee, S. Maity and C. H. Mastrangelo. Sensors, 21(4), 1253, 2021.

34. S. Firdous, S. Anwar and R. Rafya, Laser Phys. Lett. 15, 065602, 2018.

35. Homola, J.; Piliarik, M. Surface Plasmon Resonance (SPR) sensors, in Springer Series on Chemical Sensors and Biosensors: Surface Plasmon Resonance Based Sensors, Edited by Homola, J.; Springer Berlin, Heidelberg, 2006.

36. Y. Zeng, R. Hu, L. Wang, D. Gu, J. He, S. Y. Wu, H. P. Ho, X. Li, J. Qu, B. Z. Gao and Y. Shao, Nanophotonics, 6 (5), 1017, 2017.

37. K. Bremer and B. Roth, Opt. Express 23, 17179, 2015.

38. H. Yoo, J. Shin, J. Sim, H. Cho, S. Hong, Biosens. Bioelectron., 168, 112561, 2020.

39. T. Xue, W. Liang, Y. Li, Y. Sun, Y. Xiang, Y. Zhang, Z. Dai, Y. Duo, L. Wu, K. Qi, B. N. Shivananju, L. Zhang, X. Cui, H. Zhang and Q. Bao, Nature Commun., 10, 28, 2019.

40. J. Yuan, R. Duan, H. Yang, X. Luo and M. Xi, Inter. J. Nanomed., 7, 2921, 2012.

41. B. A. Prabowo, A. Purwidyantri and K. C. Liu, Biosensors., 8(3), 80, 2018.

42. M. Li, R. Li, C. Li, N. Wu, Front. Biosci., S3, 1308, 2011.

# Biosorption of Cs (I): Utilization of an eco-friendly adsorbent Dry Cowdung Powder

Roshan P. Khilnani and Hemlata K. Bagla*

Dept. of Nuclear and Radiochemistry, Kishinchand Chellaram College, Vidyasagar Principal

K. M. Kundnani Chowk, Churchgate, Mumbai – 400020.

Email: hemabagla@gmail.com

**Abstract:**

Dry Cowdung Powder (DCP) – a green biosorbent, has been demonstrated for Cs(I) removal from aqueous media using radiotracer technique. 100 mesh DCP was added to Cs(I) carrier solution spiked with radioactive Cs-137. Parameters like pH, biosorbent dose, agitation speed, contact time, temperature and Cs(I) ion concentration were optimized. Industrial effluents or other polluted water bodies contain different salts in varying proportions. To analyse the effect of these salts on adsorption of Cs(I), various sodium, potassium and ammonium salts were used. DCP characteristics pre and post biosorption of Cs(I) was analysed with EDAX spectra. The investigation reports a successful Cs(I) metal removal by following the principles of green chemistry.

**Introduction**

Treatment of a liquid waste using ecofriendly techniques is the focus of modern times. As the metallic content increases, the toxicity of the effluent increases and impacts the environment severely. Cs(I) is an alkali metal like potassium which can be easily taken up by humans through the digestive tract. Cs(I) tends to concentrate in muscles due its similarity to K(I), and gets eliminated from the body fairly quickly. We have applied radiotracer technique for Cs(I) removal using Cs-137 as a radiotracer of interest as it takes major part in radioactive wastes and aqueous waste from different industries.

There are number of techniques applied over the years for separation studies, such as ion exchange, chemical precipitation, membrane process, and liquid extraction. These have certain shortcomings like partial metal removal, higher energy and reagent requirements, production of hazardous waste materials, and their disposal treatment. The biosorption technique follows green chemistry principle for effluent clean up. Biosorption is the physico-chemical interaction between dead biomass and pollutants and is faster compared to bioremediation, due to passive binding. Plant biomass and microbes like marine algae, *Rhodosporidium fluviale, Ocimum basilicum, Azolla filiculoides,* coir pith, arca shells and minerals like illite have previously been used for Cs(I) removal from different matrices [1-3]. Thus, the aim of this work is the biosorptive removal of Cs(I) using DCP for wastewater remediation.

Freely available non living biomass DCP holds natural adsorption properties owing to the presence of humic acid, fulvic acid and bile pigments, proteins and fats etc. DCP binds and concentrates metallic pollutants from the surroundings without any external energy which makes the process kinetically faster and cost effective. Radiotracer technique simplifies the process without any radiolysis effect. It requires a very small amount of radioisotope for elemental detection.

**Experimental:**

- DCP was procured from Keshav Shristi Research Centre, Bhayander, India, with size of 100 mesh and is from a single source origin which is used throughout the experimental parameters.

- The Radiotracer $^{137}$Cs(I) was obtained from BRIT (Board of Radiation and Isotope Technology, Mumbai, India). Strength of Cs tracer used was 0.25 micro curie and 1 mL of this solution was used as tracer for all experiments.

- **Batch Biosorption:** DCP in known amount was added to 15 mL of solution containing 1 mL of $^{137}$Cs(I) tracer, 1mg of Cs(I) carrier and pH adjustment was done using dil. $HNO_3$ to maintain homogeneity across all parameters for the experiment. Nitrates formed are soluble in water and would still interact with the adsorbent. And for basic range dil. NaOH was used. To achieve equilibration, the resultant solution was mechanically stirred for required time and then centrifuged. The final activity

was measured with a NaI(Tl) well-type gamma-ray spectrometer (GRS). Experimental parameters like pH (1 to 10), Cs(I) ion concentration (0.5 – 20 mg/mL), contact time (0 – 30 min), agitation speed (0 – 4000 rpm), adsorbent dose (6.67 – 46.67 g/L), temperature (283–363 K), have been optimized for developing an efficient process. The reaction mechanism was investigated by applying kinetic, isotherm and thermodynamic modelling. Reproducibility has been checked in triplicate. The percentage biosorption was calculated using following formula:

$$\% \text{ Adsorption} = \frac{A(i) - A(f)}{A(i)} \times 100 \qquad \qquad \dots(1)$$

Where, A(i) = Initial Activity, A(f) = Final Activity in supernatant

**Results and Discussion**

All parameters have been comprehensively studied in possible experimental range for optimization of all parameters.

### 1. Effect of solution pH

The overall surface charge of an adsorbent can be controlled by modifying the solution pH over a broad range. Both Cs(I) and DCP behave as oppositely charged adsorbate and adsorbent which increases the electrostatic force of attraction between them and results into biosorption of Cs(I) on DCP. The result of pH variation is shown in **Fig. 1**. As pH increases, percentage adsorption rises and attains a plateau between pH 4 to 6, this may be due to no change in the ligand binding to Cs in this pH range. It is known that DCP being heterogeneous in nature, ligand binding may change with change in pH. Optimum pH of Cs(I) sorption was found at pH 7 for the maximum bisorption of 43% of 1 mg/15mL of Cs(I) and the adsorption remains at a plateau between pH 7 to 10. More negatively charged active sites become available as pH increases, thus facilitating greater metal uptake [4]. The formation of a plateau can be attributed to the saturation in available sites for binding.

### 2. Effect of adsorbent dose

Varying the adsorbent dose from low to high amount increases the adsorption till the system achieves equilibrium due its direct proportionality to surface area available. Equilibrium is achieved after 40 g/L and further addition does not increase the biosorption due to interaction

and aggregation of adsorbent sites. Our results from **Fig. 2** suggest that by employing 40 g/L of DCP 42.89% of Cs(I) was successfully removed.

### 3. Effect of Temperature

Biosorption process has been reported exothermically [5] in nature thus temperature is an important aspect in adsorption. It is observed from **Fig. 3** that Cs(I) biosorption increases as temperature increases and is maximum at 303K. As temperature is increased further it exhibits a negative impact and a decrease in sorption was observed. The maximum thermal energy weakens the bond between Cs(I) and DCP which can further be applied for desorption studies.

Table 2 gives optimized paameters for maximum bioabsorption of Cs(I).

### 4. Effect of Salts

The effect of different organic and inorganic salts on biosorption process is an important part due to the presence of these salts in polluted waters or in industrial effluents. Biosorption experiments were performed at different salt concentration like 10, 25, 50 and 100 mg, keeping the optimized parameters constant. Biosorption behaviour was seen in **Table 1** with different salts in which some salts supress adsorption with low concentration and some act as non-intereferring at high concentration of 100 mg.

An increased ligand concentration decreases the adsorption because of a stable metal-ligand complex being formed or competition between the metallic ion and ligand for sorption sites on the adsorbent. 100 mg thiourea and 50 mg acetate and citrate were non-interfering hence these salts can be used for separation of Cs(I) from other metallic ions which get suppressed by these ligands. At a concentration of 10 mg, chloride, chromate, dichromate, phosphate and nitrite salts interfered with Cs(I) biosorption. Their effect was overcome by doubling the DCP dosage. For separation studies, these salts may be employed as masking agents depending on their affinities for other metal ions.

### 5. Thermodynamic Parameters

The spontaneity of the reaction has been analysed using thermodynamic parameters. A negative change in Gibbs free energy $\Delta G^0$, suggests the spontaneity of a chemical reaction. And both energy and entropy factors must be considered to calculate $\Delta G^0$ of a process.

Reactions occur spontaneously at a given temperature if $\Delta G^0$ is negative [6–10]. $\Delta G^0$ is calculated by the equations:

$$\Delta G = \Delta H - T\Delta S \text{ [Gibbs free energy equation]} \qquad \ldots(2)$$

$$\Delta G^0 = -RT \ln K_a \text{ [Van't Hoff equation]} \qquad \ldots(3)$$

Where R = Universal Gas Constant (8.314 J/mol/K), T = Temperature (K), $K_a = C_0/C_e$ ($C_0$ = activity or conc. of adsorbed metal ion, $C_e$ = activity or conc. of metal ion left in solution at equilibrium)

The standard Gibbs free energy $\Delta G^0$ (kJ/mol), standard enthalpy change $\Delta H^0$ (kJ/mol), and standard entropy change $\Delta S^0$ (J/mol K) were calculated using the above equations.

Combining equation nos. 2 & 3 and rearranging in linear form [y = mx + c] as following

$$\ln K_a = \frac{\Delta S^0}{R} - \frac{\Delta H^0}{RT} \qquad \ldots(4)$$

The values of $\Delta H^0$ and $\Delta S^0$ were computed from the graph of Ln $K_a$ vs. $1/T$ x $10^3$ (as seen in **Fig. 4),** to be -35.93 kJ/mol and 112.95 J/mol K respectively. $\Delta G$ at 303K was -1.36 KJ/mol, thus negative value confirms the feasible and spontaneous biosorption with high preference of Cs(I) ions for DCP. $\Delta H^0$ is negative, thus the reaction is exothermic and $\Delta S^0$ is positive, which reflects the affinity of adsorbent for Cs(I) ions.

## 6. Kinetic Parameter

The kinetic biosorption data were obtained by batch experiments by varying the time of reaction from 0 to 30 min. Lagergren pseudo-first-order, Ho & McKay pseudo-second-order and intraparticle diffusion model have been used. From these models, Ho & McKay pseudo-second-order model was the best-fitting [11–13].

The Kinetic data obtained was applied to Ho & McKay pseudo-second-order model as expressed in the equation given below:

$$\frac{dq_t}{dt} = K_2 (q_e - q_t)^2 \qquad \ldots(5)$$

Rearranging Equation 5 in linear form as [y = mx + c]

$$\frac{t}{q_t} = \frac{1}{K_2\, q_e^2} + \frac{1}{q_e} t \qquad \qquad \ldots(6)$$

Where,

t = time (min)

$q_t$ = amount of metal (mg) adsorbed per gm of adsorbent at time (t)

$q_e$ = Maximum adsorption capacity

$K_2$ = rate constant (g mg$^{-1}$ min$^{-1}$)

The graph of t/qt versus t is shown in **Fig. 5**. The constants $K_2$ = -13.75 g mg$^{-1}$ min$^{-1}$ and $q_e$ = 0.63 mg/g have been calculated from the graphical equation. The correlation coefficients $R^2$ value 0.9995 was close to 1, thus pseudo-second-order kinetics fit the system and the rate-limiting step may be chemical adsorption involving valent forces through sharing or the exchange of electrons between the DCP and monovalent Cs(I) ions.

## 7. Isotherm profile

Most mathematical biosorption models used in literature describe simple Langmuir or Freundlich sorption isotherms, where the metal binding is determined as a function of its equilibrium concentration in the solution, without reference to pH or competing ions in the same solution system. For this study, both models were applied to the data obtained[6,14–20].

Langmuir isotherm model gives the monolayer formation of adsorbate on the outer surface of adsorbent, after this surface interaction no further adsorption occurs and sytem achieves equilibrium. Thus, it represents the equilibrium distribution of metal ions between the solid and liquid phases.

Linear form [y = mx + c] can be expressed as

$$\frac{1}{q_e} = \frac{1}{K_L\, Q_0}\, \frac{1}{C_e} + \frac{1}{Q_0} \qquad \qquad \ldots(7)$$

Where,

$C_e$ = the equilibrium concentration (mg/dm$^3$)

$q_e$ = the amount of metal ion sorbed (mg/g)

$Q_0$ = $q_e$ for a complete monolayer (mg/g) = Maximum adsorption Capacity

$K_L$ = Langmuir biosorption equilibrium constant (dm$^3$/mg)

$R_L$ is an equilibrium parameter which indicates nature of adsorption, it is an essential feature of the Langmuir model which follows the given characteristics:

if $R_L > 1$ process is Unfavourable,

if $R_L = 1$ process is Linear,

if $0 < R_L < 1$ process is Favourable,

if $R_L = 0$ process is Irreversible[7].

Where $R_L$ is calculated using the equation:

$$R_L = \frac{1}{1 + K_L C_0} \qquad \qquad …(8)$$

Where,

$C_0$ = initial concentration (mg/dm$^3$)

$K_L$ = the constant related to the energy of adsorption (Langmuir Constant).

$R_L$ = the value indicates the adsorption nature

Freundlich isotherm can be applied for both monolayer chemisorption process and multilayer adsorption. The Freundlich isotherm can be derived assuming a logarithmic decrease in the enthalpy of sorption with the increase in the fraction of occupied sites. It is expressed as following:

$$q_e = K_F C_e^{1/n} \qquad \qquad …(9)$$

Linear form expressed as [y = mx + c]

$$\log q_e = \log K_F + \frac{1}{n} \log C_e \qquad \qquad …(10)$$

$K_F$ acts as an indicator of adsorption capacity. Similarly, 1/n is an indicator of the strength of adsorption, if 1/n < 1 it indicates chemical adsorption and explains favourable adsorption at low adsorbate concentration, if 1/n > 1 it suggests cooperative adsorption and strong attraction between the adsorbate and adsorbent even with high concentration. If n<1 or n>1 it implies chemical and physical adsorption respectively.

The regression coefficient for Langmuir isotherm for Cs(I) biosorption found to be 0.6823 which prove that the system does not fit for thr same. From **Fig. 6,** Freundlich constant Kf was 0.12, 1/n value was 0.4769, and n was 2.10, with $R^2 = 0.9096$. The best-fitting isotherm

to explain the nature was Freundlich model which indicates that biosorption involves chemical bonding between DCP and Cs(I) and is favourable at low Cs(I) concentration.

### 8. EDAX Spectra pre and post adsorption

Characterization of the biosorbent is an important step in understanding metal ion and biosorbent bonding mechanism. To study this part, the EDAX spectra has been analysed pre and post sorption. The results suggest the presence of K, Si, Zn, Fe, Ti, Mn on the matrix of DCP from **Fig. 7**. After biosorption, the presence of Cs(I) can be seen on the matrix of DCP along with other elements which indicates the mechanism does not follow ion exchange procedure. The kinetic calculations show that the reaction follows Ho & McKay pseudo-second-order model which suggests a chemical interaction between metal ion and sorption sites of DCP.

**Conclusions**

All the parameters have been comprehensively studied in possible experimental range for optimization. For biosorption of 1 mg Cs(I) with DCP at solution pH 7, time of contact 5 min, with 40 g/L of DCP, agitation speed 2000 rpm, at 303K, the removal efficiency is about 40-45 %. The modelling parameters were also studied with optimized parameters. Cs(I) is a very weak Lewis acid and has a low tendency to interact with ligands in general, thus making its biosorption a challenging prospect. Study of salts was undertaken to understand their interference and to compile them as possible masking agents for separation studies. The kinetic, thermodynamic and isotherm studies suggested that sorption on DCP was a chemical interaction between Cs(I) and sorption sites of DCP and is a spontaneous exothermic process which was also confirmed by the EDAX studies. The study provides collective data on biosorption of Cs(I) using an eco-friendly biosorbent along with the interference of different salts.
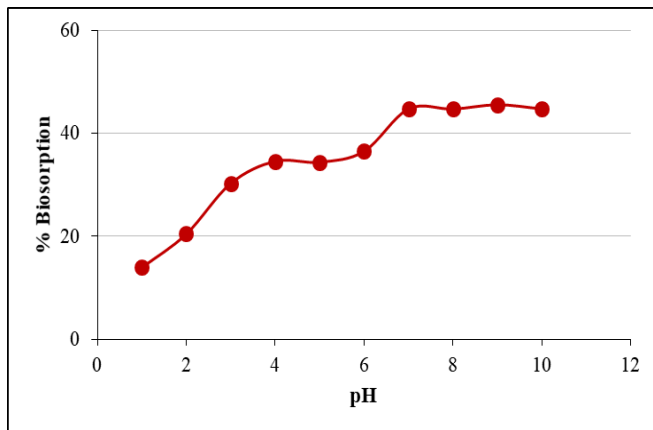
**Figures:**



**Fig. 1:** Effect of solution pH on biosorption of Cs(I)
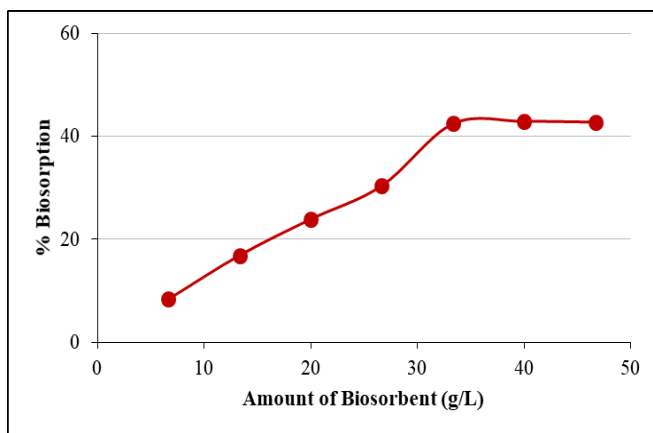


**Fig. 2:** Effect of adsorbent dose on biosorption of Cs(I)
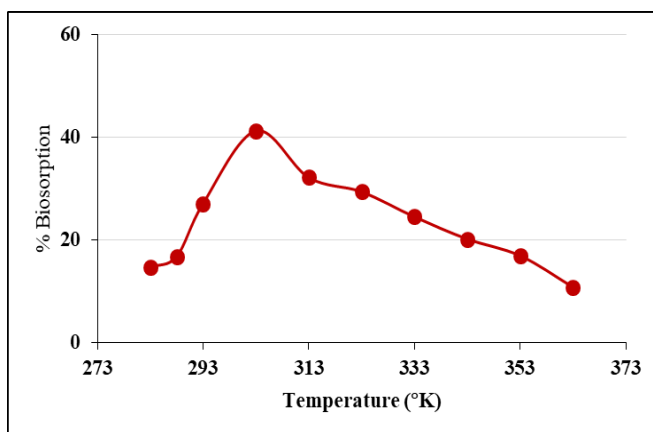


**Fig. 3:** Effect of Temperature on biosorption of Cs(I)
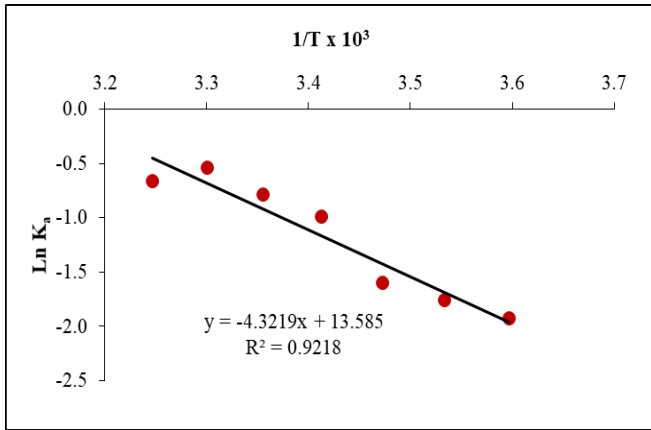
**Fig. 4:** Thermodynamic graph of Ln $K_a$ vs 1/T x $10^3$
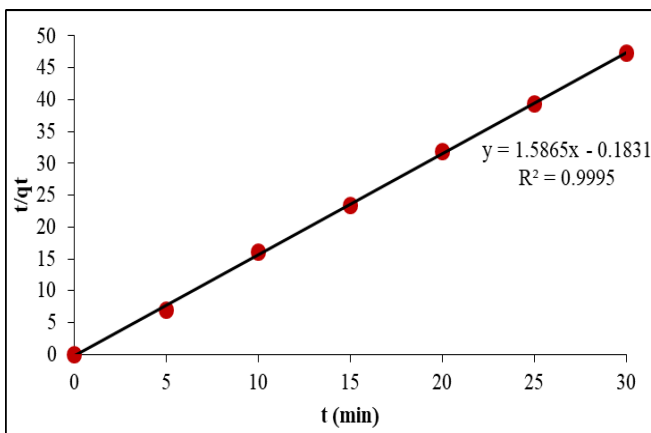


**Fig. 5:** Ho & McKay pseudo-second order Plot of $t/q_t$ vs t
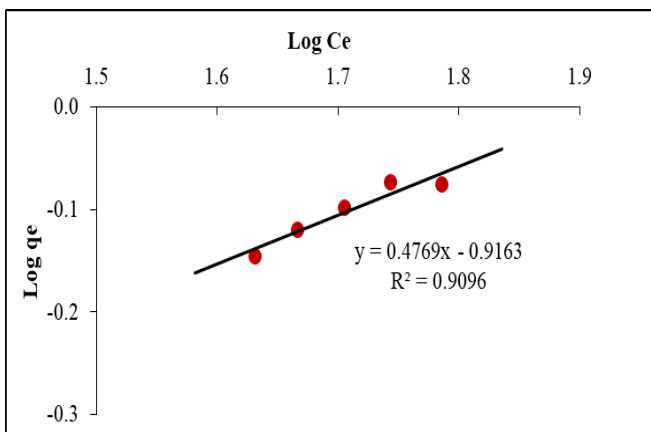


**Fig. 6:** Freundlich Isotherm Plot of log $q_e$ versus log $C_e$
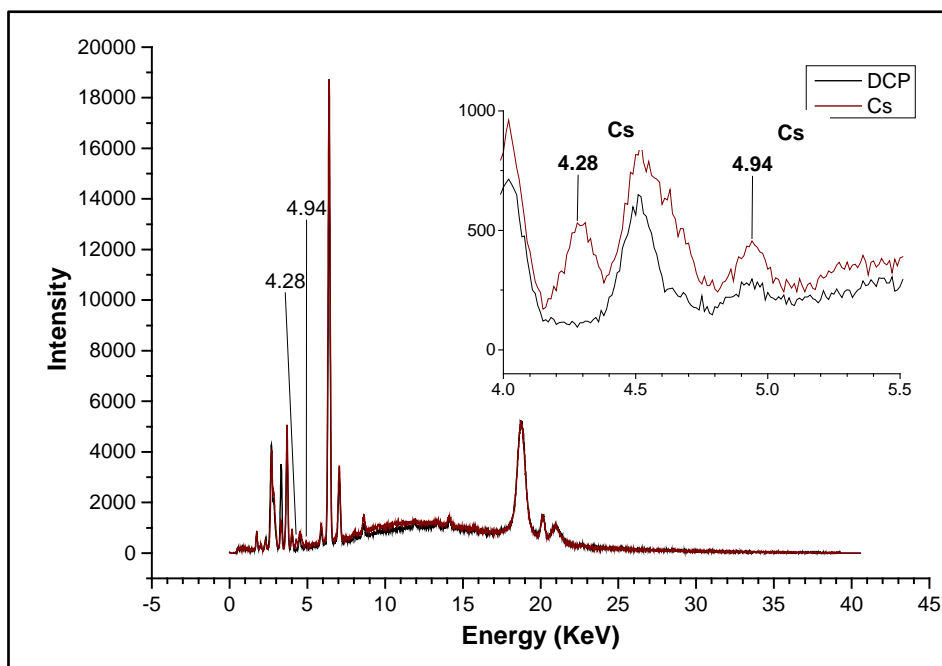
**Fig. 7:** EDAX spectra of Intensity versus Energy (KeV) of DCP pre and post adsorption of Cs(I)

**Tables:**

**Table 1:** Effect of salts on biosorption of Cs(I) under the optimized conditions

| Amount of Salt in mg | | Salts under study |
|---|---|---|
| 100 | Non-interfering | Thiourea |
| 50 | Non-interfering | Acetate, Citrate |
| 25 | Non-interfering | Sulphate, Nitrate, Iodate, Carbonate, Thiosulphate, EDTA, Tartarate, Oxalate |
| 10 | Non-interfering | Hydroxide, Chlorate, Fluoride, Bicarbonate, Bromide, Sulphite |
| 10 | Interfering | Chloride, Chromate, Dichromate, Phosphate, Nitrite |

**Table 2 Optimized parameters for maximum Biosorption of Cs(I)**

| | |
|---|---|
| pH | 7.0 |
| Adsorbent dose | 40 g/L |
| Agitation Speed | 2000 rpm |
| Contact time | 5 min |
| Temperature | 303K |
| **% Biosorption** | **42 – 45 %** |

**References**

1. Jalali-Rad R, Ghafourian H, Asef Y, Dalir ST, Sahafipour MH, Gharanjik BM. *J Hazard Mater*. 116(1–2).125, 2004.

2. Parab H, Sudersanan M. ,*Water Res*. 44(3), 854, 2010.

3. N.J. Comans R, Haller M, De Preter P. ,*Geochim Cosmochim Acta*. 55(2), 433, 1991.

4. Ajmal M, Rao RAK, Ahmad R, Ahmad J., *J Hazard Mater*. 79(1-2), 117, 2000.

5. Derco J, Vrana B. Introductory Chapter: Biosorption. In: *Biosorption*. 2018.

6. Ho Y-S, Ofomaja AE. ,*Biochem Eng J*. 30(2), 117, 2006.

7. Jaikumar V, Ramamurthi V. ,*Int J Chem*. 1(1), 2 2009.

8. Liu Y, Liu YJ. ,*Sep Purif Technol*. 61(3), 229, 2008.

9. Aksu Z. *Process Biochem*. 38(1), 89, 2002.

10. Aly Z, Luca V. ,*J Radioanal. Nucl Chem*. 295(2), 889, 2013.

11. Lagergren S. ,*Kungliga SvenskaVetenskapsakademiens Handlingar*. 24(4), 1, 1898.

12. Ho YS, Mckay G., *Process Biochem.* 34,451, 1999.

13. Ho, McKay. *Adsorpt Sci Technol*. 20(8), 797, 2002.

14. Limousin G, Gaudet JP, Charlet L, Szenknect S, Barthe V, Krimissa M., *Appl Geochemistry*. 22, 249, 2007.

15. Foo KY, Hameed BH,, *Chem Eng J*. 156(1), 2, 2010.

16. Allen SJ, Mckay G, Porter JF.*J Colloid Interface Sci*. 280(2), 322, 2004.

17. Malek A, Farooq S. *AIChE J*. 42(11), 3191, 1996.

18. Bulut E, Özacar M, Şengil İA.,*Microporous Mesoporous Mater*. 115(3),234, 2008.

19. Yuh-Shan H., *Scientometrics*. 59(1), 171, 2004.

20. Dada AO. ,*IOSR J Appl Chem*. 3(1), 38, 2012.

# A Simple and Rapid Spectrophotometric method for the determination of Iodate in table salt samples using Pyrogallol red dye

P.S. Kulkarni

Post-graduate and Research Centre, Department of Chemistry, MES, Abasaheb Garware College Pune 411004

Email: psk.agc@mespune.in

**Abstract:**

A simple and rapid spectrophotometric method for the determination of iodate in table salt samples has been standardized using the oxidation reaction of iodate with pyrogallol red dye in sulphuric acid medium. The determination of iodate was done by measuring the decrease in absorbance of pyrogallol red dye at 470 nm. A standard calibration curve was prepared, for iodate concentrations in the range of 0.05 µg mL$^{-1}$ to 5 µg mL$^{-1}$. The effect of NaCl and I$^-$ interference on iodate determination has been studied. The kinetics of the reaction between pyrogallol red and iodate has also been studied. The oxidation reaction was found to be first order with respect to iodate concentration. The method has been used for the determination of iodate in 10 different brands of locally available common salt samples.

**Key Words:** Iodate, Table salt, Pyrogallol

## Introduction:

Iodine is an important constituent of the thyroid hormones. These hormones regulate the rate of metabolism and affect the growth and functioning of many systems in the human body[1]**.** Low amounts of thyroid hormones in the blood due to iodine deficiency, stimulates the abnormal growth of the thyroid gland causing goiter[2]**.** Iodine deficiency can be controlled through the addition of iodized salt in cooked food. Iodization of salt is done by adding 20-80 of iodine per kilogram of salt in the form of sodium or potassium salt of iodide or iodate. In hot climatic conditions like India, iodide is easily oxidized to I$_2$ and then lost by evaporation, while iodate is more stable, also the chemical stability of iodate is more in alkaline conditions than iodide[3]**.** Hence, potassium iodate is most commonly used for the fortification of salt in

India. In order to know the daily dietary intake of iodine it is essential to know the iodate concentration in various brands of commonly available salt samples.

Survey of the literature reveals that many analytical techniques have been used for the determination of iodate in salt samples. The most commonly used technique is spectrophotometry where iodate reacts with several chromogenic reagents to form colored species[4-7]. Iodate has also been oxidized to iodine in acidic medium which reacts with dyes to give spectrophotometric signals[8]. A spectrofluorometric method for determination of iodate with rhodamine 6G has been developed by studying the fluorescence quenching of rhodamine 6G at 540 nm[9]. Trace levels of iodate have been determined by gas chromatography mass spectrometry (GC-MS) by its reduction to iodide using ascorbic acid followed by its oxidation to iodine and its derivatization to 4-iodo-2,6-dimethyphenol[10,11]. Iodate has also been estimated in salt using ion chromatography with conductivity detection[12]. This method requires a pretreatment for the removal of large excess of chloride. Flow injection amperometry has also been used for the determination of iodate in iodized table salt[13]. The electrocatalysis of iodate reduction at tungsten oxide films has been used for the determination of iodate content in table salt samples[14]. A rapid chemiluminescence method has been developed for the determination of iodate based on its reaction with iodide in acidic condition[15]. Trace amounts of iodate and iodide in table salt samples have been estimated by Epithermal Neutron Activation Analysis using Cadmium shielding and boron carbide[16]. A flow injection spectrophotometric method has been standardized for the determination of iodate and per-iodate by their reaction with pyrogallol red in acidic media[17]. A simultaneous kinetic spectrophotometric determination of per-iodate and iodate has been done based on their reaction with pyrogallol red in acidic media by chemometrics method[18]. In the present work the pyrogallol red dye oxidation reaction has been standardized for the determination of iodate in table salt samples. The determination of iodate was done by measuring the decrease in absorbance of pyrogallol red at 470 nm. The effect of NaCl and I$^-$ on iodate determination has been studied. The kinetics of the reaction between pyrogallol red and iodate has also been studied and the reaction was found to follow first order kinetics. The method has been used for the determination of iodate in ten different brands of locally available iodized table salt samples. The iodate concentrations in these salt samples were found to be in the range of 10-50 mg kg$^{-1}$. The novelty of this work is, in determination of Iodate with pyrogallol no pre-treatment is required and method is fairly sensitive.

**Experimental:**

**Reagents and Apparatus**

Analytical reagent grade chemicals (KI, NaCl, KIO$_3$, and H$_2$SO$_4$) were obtained from Merck. Pyrogallol red dye (C$_{19}$H$_{14}$O$_9$S) was obtained from Loba chemie, Deionized water (18 MΩ/cm) purified by model Quantum$^{TM}$ from Millipore was used throughout the present studies. A stock solution of iodate (2 mg mL$^{-1}$) was prepared by dissolving 0.61 g of KIO$_3$ in water in 250 mL volumetric flask. Pyrogallol red dye solution was prepared by dissolving 9 mg of the dye in a mixture of 1:1 MeOH/H$_2$O in a 100 mL volumetric flask. UV-Vis spectra of the samples and standard solutions were recorded using a UV-Vis Spectrophotometer UV-1650 PV from Shimadzu. The scanning rate was 200 nm min$^{-1}$ and the path length of the quartz cells was 1cm.

**Method:**

**Preparation of calibration curve**

For the preparation of a standard linear calibration curve iodate solutions were prepared in the concentration range of 10-1000 µg mL$^{-1}$ by necessary dilutions from the stock solution. For the concentration range of 0.2-20 µg of iodate, a 20 µL volume of iodate solution 10-1000 µg mL$^{-1}$ was added to a mixture of 1mL dye solution and 1mL of 0.05 M H$_2$SO$_4$. The total volume of this solution was made to 4 mL with de-ionized water. All the solutions were kept for a period of 5 min at 25$^o$C after addition of IO$_3^-$ solution to it and the decrease in absorbance of pyrogallol red dye at 470 nm was measured. A blank sample was used in the calibration set where all the reagents except iodate solution were added.

**Optimization of Experimental parameters**

The concentration of sulphuric acid required for the oxidation of pyrogallol red by iodate was optimized by adding 1 mL of H$_2$SO$_4$ of concentration varying between 0.01 M to 0.07 M to 1mL of dye solution. The total volume of all the solutions was made to 4 mL with deionized water. A 20 µL volume of iodate solution (400 µg mL$^{-1}$) was added to all the solutions. All the solutions were kept for a period of 5 min and the absorbance spectra were recorded. For the optimization of the concentration of pyrogallol red dye 1mL of 0.05 M H$_2$SO$_4$ was added to 1mL solutions of pyrogallol red having concentration in the range of 0.01 mg mL$^{-1}$ to 0.12 mg mL$^{-1}$ respectively. After addition the same procedure as described above was followed and the absorbance spectra were recorded

**Kinetics of the Reaction**

The kinetics   of the oxidation reaction of pyrogallol red due to presence of iodate was studied by taking 1mL of dye solution, 1mL of 0.05 M $H_2SO_4$ and 2mL of distilled water in a quartz cuvette. 20 µL of iodate solution (120 µg $mL^{-1}$) was added to this cuvette and the decrease in absorbance of pyrogallol red at 470 nm was recorded as a function of time at an interval of every one min for a period of 15 min. The same procedure was repeated for each of the iodate solutions over a concentration range of 200 – 800 µg $mL^{-1}$ of iodate solution. The decrease in absorbance value at 470 nm was plotted as a function of time in each case and the values of the rate constants were calculated. The order of the reaction with respect to iodate was also determined.

**Effect of NaCl and I⁻ on oxidation of pyrogallol red by iodate**

The effect of NaCl on the oxidation of pyrogallol red dye was studied by varying the amount of Analytical reagent grade NaCl (0-200 mg) in the solution containing a mixture of 1mL of acid solution and 1 mL of dye solution. The final volume of the solution was made 4 mL in all the cases by the addition of deionized water. 20 µL of iodate solution (200 µg $mL^{-1}$) was added to all the solutions. All the solutions were kept for a period of 5 min and the decrease in absorbance of pyrogallol red dye at 470 nm was measured.

To study the interference due to I⁻ on the oxidation of pyrogallol red dye varying amounts of iodide (0- 10 µg) were added to the solution containing a mixture of 1mL acid and 1 mL dye solution. After addition of the iodide solution the same procedure as described above for NaCl was followed and the absorbance spectra were recorded

**Estimation of iodate contents in commercially available iodized salt samples**

About 10 g of locally available salt samples containing iodate were removed from packets and homogenized using mortar and pestel. These homogenized samples were used for the determination of iodate in the salt samples by pyrogallol red dye method. 1g of the homogenized salt sample was dissolved in 50 mL of deionized water. 1 mL of dye solution and 1mL of 0.05 M $H_2SO_4$ were taken in a quartz cuvette. To this solution 2.20 µL of above salt sample solution was added and the decrease in absorbance at 470 nm was recorded after a time period of 5 min. The concentration of iodate in the salt samples was calculated by using the standard calibration curve.

**Results and Discussion**

A method for the   kinetic determination of iodate and periodate based on their reaction with pyrogallol red in acidic media has been standardized by Ghasemi et al and applied for the

determination of iodate in water samples[18]. In the present work the same reaction of pyrogallol red oxidation by iodate in acidic media has been used for the determination of iodate in locally available table salt samples.

**Standard Calibration Curve**

Pyrogallol red (Pyrogallolsulfonephthalein), $C_{19}H_{12}O_8S$ is a complexing indicator (Fig 1). The solution of pyrogallol red prepared in alcohol-water mixture shows absorbance maxima at 470 nm.  Pyrogallol red gets oxidized by iodate in acidic media to form a colourless product. The oxidation reaction of pyrogallol red with iodate can be monitored by the decrease in absorbance of pyrogallol red at 470 nm. A linear calibration curve was obtained for iodate concentrations in the range of 0.05 µg mL$^{-1}$ to 5 µg mL$^{-1}$. The change in absorbance value at 470 nm with respect to the blank absorbance value at the same wavelength has been plotted as a function of amount of Iodate in the reaction mixture and is shown in the (Fig 2).  It can be seen from the figure that the plot is a straight-line having equation    [y = 0.0735 x + 0.0003 $R^2$ = 0.9885] indicating a linear decrease in the absorbance value of pyrogallol red with increase in concentration of iodate. The detection limit calculated from the 3σ value of blank is 0.04 µg $IO_3^-$.

**Effect of different parameters on the oxidation of pyrogallol red**

The oxidation of pyrogallol red by iodate is found to be greatly affected by the acidity of the reaction mixture. The effect of acid concentration on the oxidation of pyrogallol red was studied by varying the concentration of $H_2SO_4$ from 0.01 M to 0.07 M and measuring the change in absorbance of pyrogallol red at 470 nm. It was found that the change in absorbance value increases rapidly for acid concentration from 0.01 to 0.04 M. The change in absorbance value remains almost constant beyond acid concentration of 0.05 M. The acid concentration was therefore kept 0.05 M for further experiments. The results were found to be in agreement with those observed by Ghasemi et al[18].

The effect of the concentration of pyrogallol red on the oxidation rate was studied by varying the concentration of the dye between 0.01 mg mL$^{-1}$ to 0.12 mg mL$^{-1}$. It was found that the change in absorbance increases upto a dye concentration of 0.09 mg mL$^{-1}$ beyond which it remains fairly constant. The concentration of the dye was kept 0.09 mg mL$^{-1}$ for further experiments.

**Kinetics of the oxidation reaction of pyrogallol red with iodate**

The kinetics of the oxidation reaction of pyrogallol red with iodate was studied by measuring the decrease in absorbance at 470 nm due to addition of varying amounts of iodate to it as a

function of time. The concentration of pyrogallol red was kept fixed (0.09 mg mL$^{-1}$ and the concentration of iodate was varied between 2.4 µg to 16 µg. The absorbance spectra of the pyrogallol solution were monitored after an interval of every 1 min after the addition of iodate solution to it. The absorbance value of pyrogallol red was found to decrease rapidly during the first five minutes of the reaction. It was observed that the absorbance of pyrogallol red reached an optimum value after a period of 6-7 min after which there is no further change in the absorbance value (Fig 3). The absorbance value of pyrogallol red at any interval of time is directly proportional to the concentration of unreacted iodate at that time instant. Using these absorbance values the rate constant for the reaction with respect to iodate was calculated for each concentration of iodate. The rate constant values calculated from the first order equation showed constant values indicating the order of the reaction to be 1. The average value of the first order rate constant calculated from the equation in the present studies is $3.69 \times 10^{-2}$ min$^{-1}$. A plot of absorbance value of pyrogallol red proportional to the residual concentration of dye after addition of 2.4 µg of iodate as a function of time is given in (Fig 4). It can be seen from the figure that the plot gives best linear points suggesting the order of the reaction to be one. The equation for the plot is [y = -0.0152x - 0.0903 R2 = 0.9771]. The slope of this plot is -0.0152. The rate constant value from the slope of the plot is $3.50 \times 10^{-2}$ min $^{-1}$. Fig 5 shows oxidation of pyrogallol red with Iodate.

**Estimation of iodate in commercially available iodized salt samples**

Since the method in the present work has been applied to iodate determination in table salt samples the effect of NaCl on the oxidation of pyrogallol red dye by iodate was studied. It was observed that there was no significant change in the absorbance of pyrogallol red dye at 470 nm due to presence of NaCl upto 200 mg (Fig 6). This suggests that the method can be used without any interference for iodate determination in iodized salt samples. In some countries iodide is added as an alternative to iodate for the iodization of common salt. However, in India iodate is preferentially added over iodide for iodization of salt. The presence of iodate in some locally available table salt samples has been determined and reported in our previous work[19]. The effect of I$^-$ on the oxidation of pyrogallol red by iodate was studied and the studies indicated that the presence of iodide upto 1µg did not interfere in the iodate determination. Above 1µg iodide showed interfere in the iodate determination.

The iodate contents in ten different commonly consumed brands of iodized salt samples were determined in the present work. The results obtained are summarized in table I. It can be seen that the iodate contents obtained are in the range of 10-50 ppm. The iodine contents in all the

brands were more than that quoted by the manufacturer except for Brand-9. The results suggest that the consumption of these brands can provide adequate amount of iodine and prevent deficiency.

**Conclusions**

The present work demonstrates a simple and rapid spectrophotometric method for the determination of iodate in table salt samples using pyrogallol red dye method. The method does not require sophisticated equipment and can be easily used for the quick screening of a large number of salt samples for iodate in any laboratory.

**Acknowledgements**

Author would like to thank Prof. N.S. Rajurkar Former Professor and Head, Department of Chemistry and Former Head, Department of Environmental Science, Savitribai Phule Pune University for her guidance during present work and Head Department of Chemistry, Savitribai Phule Pune University for providing infrastructure for the present work.

**Figures:**
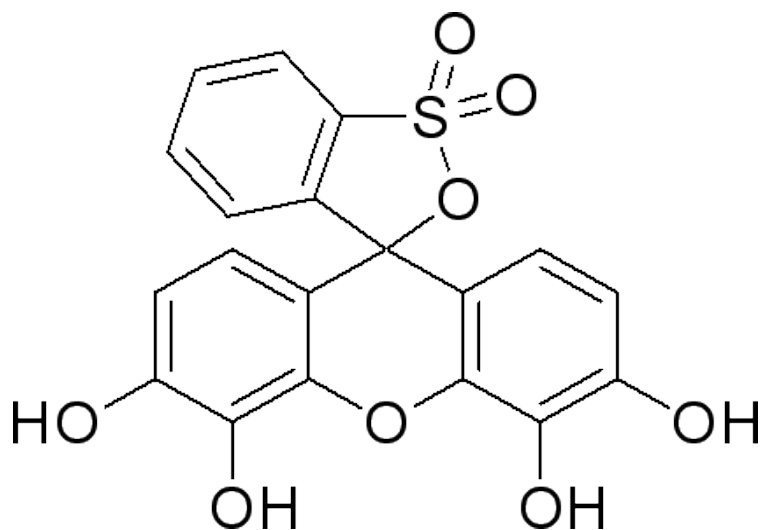


**Fig 1:** Structure of Pyrogallol red dye.
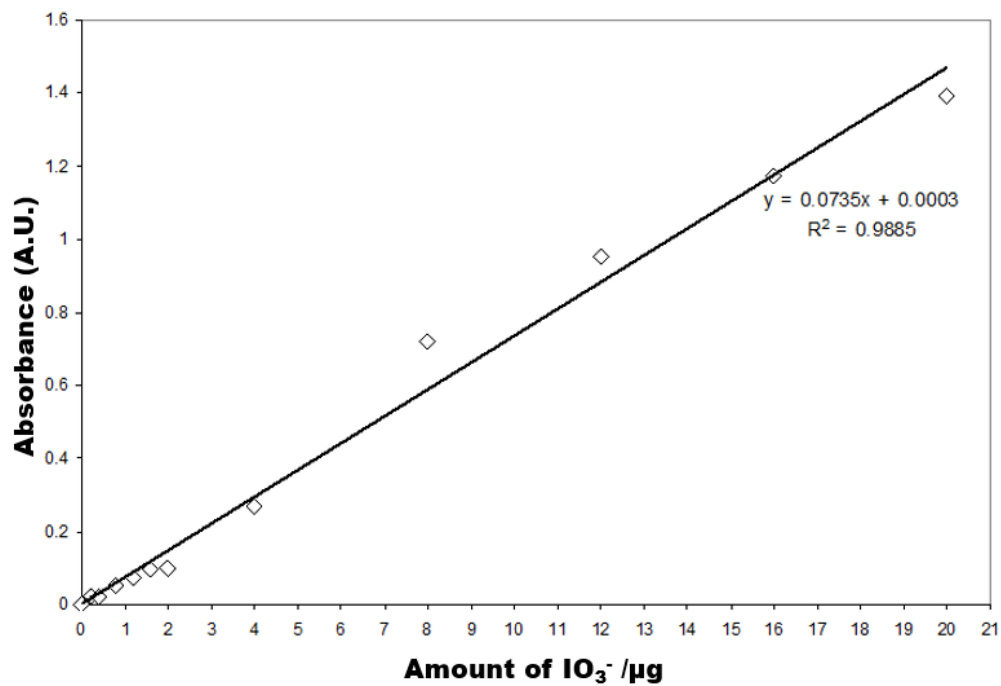
**Fig 2:** Variation of change in absorbance of pyrogallol red at 470 nm as a function of amount of Iodate
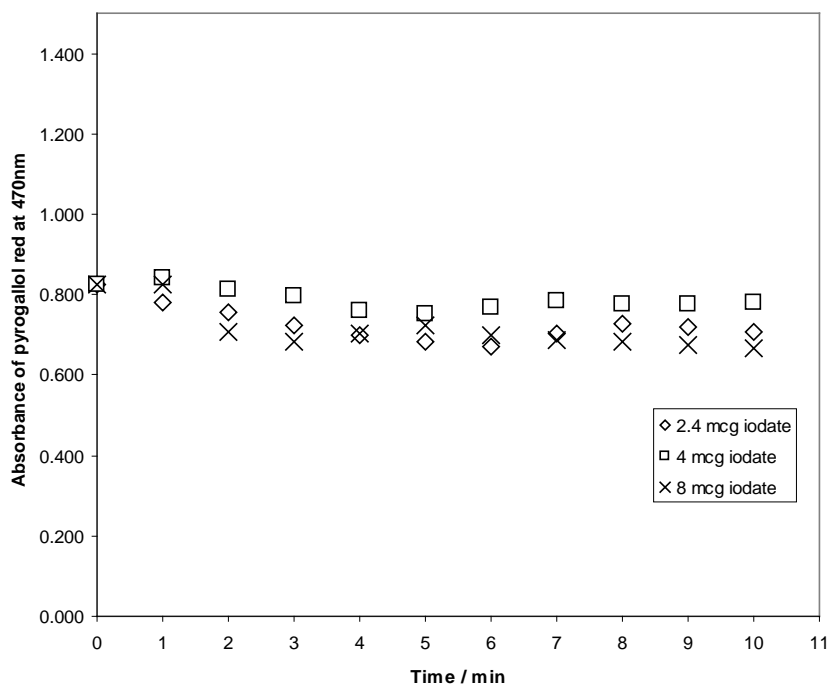


**Fig 3:** Kinetics of the oxidation of pyrogallol by Iodate

The chart shows a plot with y-axis labeled "log (A-X)" ranging from 0 to -0.2, and x-axis labeled "Time / min" ranging from 0 to 7. The trend line equation is:

$$y = -0.0152x - 0.0903$$
$$R^2 = 0.9771$$
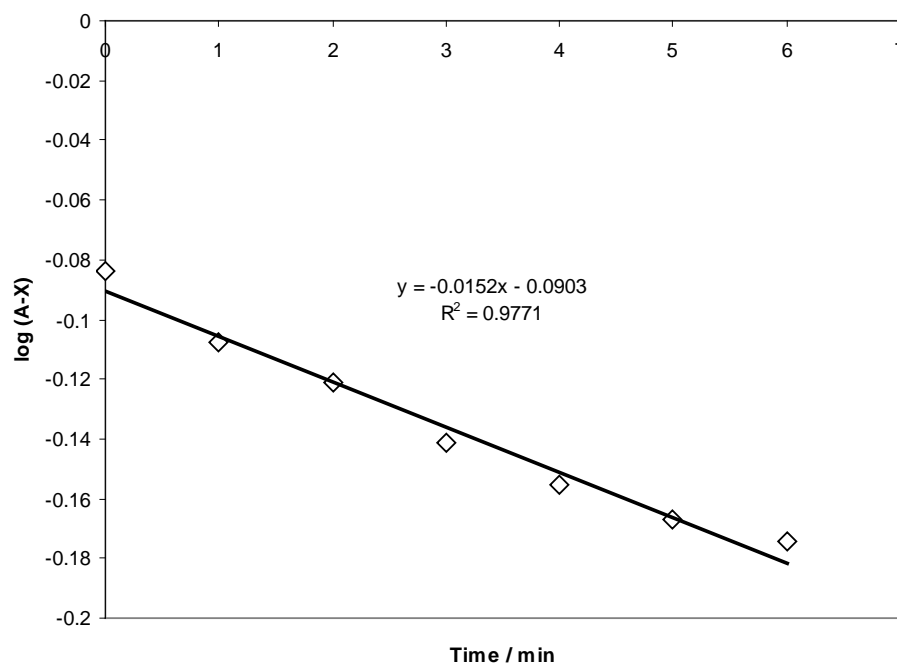
**Fig 4:** Plot of Absorbance of unreacted pyrogallol red as a function of time.
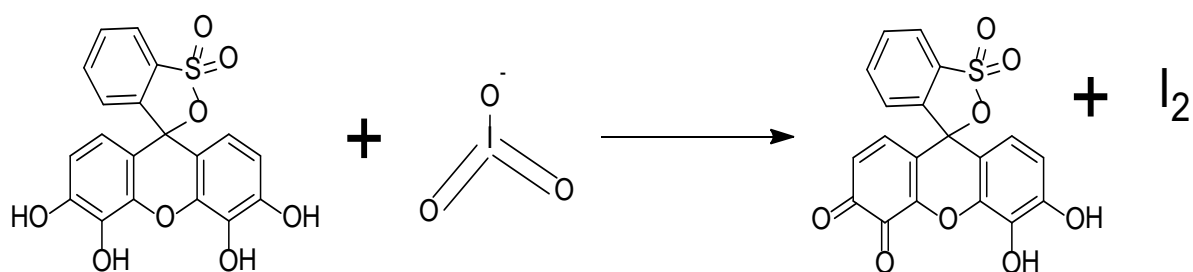


**Fig 5:** Oxidation of pyrogallol red by Iodate
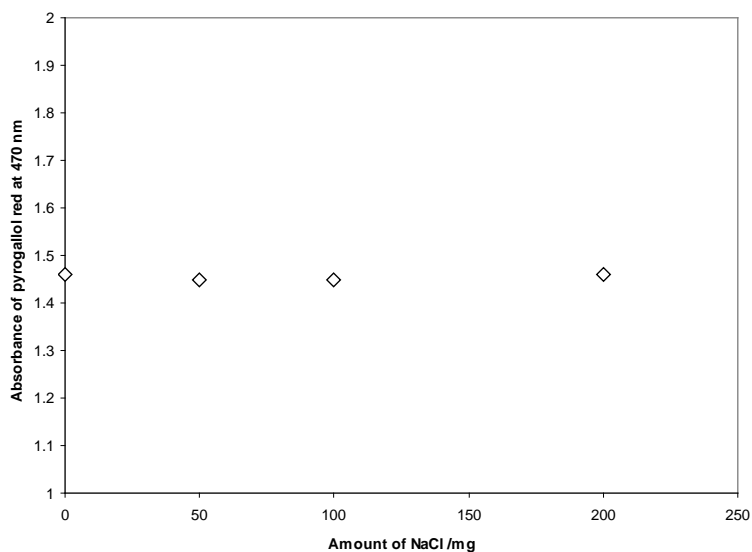
**Fig 6:** Effect of NaCl on oxidation reaction of pyrogallol red with Iodate

**Tables:**

**Table 1:** Determination of iodate content in different iodized salt brands by pyrogallol red method.

| Iodized salt Brand | Iodate content / mg kg$^{-1}$ | Minimum Iodate content Quoted on packet / mg kg$^{-1}$ |
|---|---|---|
| Brand-1 | $28.9 \pm 0.1$ | 15 |
| Brand-2 | $48.49 \pm 0.2$ | 30 |
| Brand-3 | $17.45 \pm 0.1$ | 15 |
| Brand-4 | $17.58 \pm 0.1$ | 15 |
| Brand-5 | $24.34 \pm 0.1$ | 15 |
| Brand-6 | $26.45 \pm 0.2$ | 15 |
| Brand-7 | $32.56 \pm 0.2$ | 30 |
| Brand-8 | $15.43 \pm 0.1$ | 15 |
| Brand-9 | $11.32 \pm 0.1$ | 15 |
| Brand-10 | $25.63 \pm 0.2$ | 15 |

**References**

1. S. Sorrenti, E. Baldini, D. Pironi, A. Lauro, V. D'Orazi, F. Tartaglia, D. Tripodi, E. Lori, F. Gagliardi, M. Praticò, Nutrients, 13, 4469, 2021.

2. B. Hetzel, Lancet, 2, 1126, 1983.

3. G. Arroyave, O. Pineda, N. Scrimshaw, Bull WHO, 14, 183, 1956.

4. A.Michael, G. Samantha, P. Sebastián, Anal.Methods, 12, 205, 2020.

5. C. Pasha, B. Narayana, Acta Chim Slov, 53, 77, 2006.

6. H. Galiga, F. Sevilla, J Food Compost Anal, 110, 104558, 2022.

7. M. Gupta, A. Dsouza, J Food Compost Anal, 87, 103396, 2020.

8. X. Zhihai, Z. Jingchan, Talanta, 63, 339, 2004.

9. A. Liang, Z. Jiang, B. Zhang, Q. Liu, J. Ln, X. Lu, Analytica Chimica Acta 530, 131, 2005.

10. H. Shin, Y. Oh-Shin, J. Kim, J. Ryu, J. Chrom. A, 732, 327, 1996.

11. P. Das, M. Gupta, A. Jain, K. Verma, J Chromato. A, 1023, 33, 2004.

12. S. Kumar, B. Maiti, P. Mathur, Talanta, 53, 701, 2001.

13. J. Jakmunee, K. Grudpan, Anal. Chim.Acta., 438, 299, 2001.

14. J. Rocha, T. Ferreira, R. Torresi, M. Bertotti, Talanta, 69, 148, 2006.

15. O. Zui, A. Terletskaya, Fresenius. J. Anal. Chem, 351, 212, 1995.

16. B. Nyarko, Y. Armoh, S. Osae, E. Akaho, S. Sampong, B. Maakuu, J Radio anal and Nucl Chem, 251, 281, 2002.

17. A. Ensafi, M. Chamjangali, Spectrochimica acta Part A, 58, 2835, 2002.

18. J. Ghasemi, S. Saaidpour, A. Ensafi, Anal. chim acta,. 508, 119, 2004.

19. P. Bhagat, A. Pandey, R. Acharya, V. Natrajan, N. Rajurkar, A. Reddy, Anal. Bioanal. Chem, 391, 1081, 2008.

# Determination of Lutetium In Radiopharmaceutical Samples Using High Resolution ICP-AES Technique

V.C. Adya[1+*], Arijit Sengupta[1], Sudipta Chakraborty[2], K.Vimalnath[2] and S. K. Thulasidas[1+]

[1]Radiochemistry Division, [1+]Radiochemistry Division (former), [2]Radiopharmaceutical Division

Bhabha Atomic Research Centre, Mumbai, India

*E-mail: vcadya@rediffmail.com

**Abstract:**

An analytical method was developed for the determination of Lutetium in dilute nitric acid medium using high resolution ICP-AES analytical technique. These studies were required for the determination of Lutetium contents in radiopharmaceutical samples. For the patients suffering from cancers, ^{177}Lu DOTA-TATE peptide receptor radionuclide therapy is used. This necessitates the use of ^{177}Lu and obviously the quantification of Lutetium for its efficient application during medical therapy which is used for the preparation of the patients suffering from cancers. Due to short half life of ^{177}Lu of 6.67 days, it is most likely to get added up with Hf, as it is build up on storage, the undesired impurity element. Hence the effect of Hf on the determination of Lu was studied. Subsequently seven actual samples of ^{177}Lu were analysed for Lu contents after taking into account Hf contribution if any.

**Key words :** Lutetium, ^{177}Lu, Hafnium, HR- ICP-AES, Radiopharmaceutical samples

**Introduction:**

Radioisotopes are being used worldwide for their applications in healthcare, industry, agriculture and research fields for many decades. For healthcare applications, the radioisotopes used are for Radiation Oncology (Teletherapy and Brachytherapy) and Nuclear Medicine (NM). NM is a special branch of medicine in which radioisotopes are used in the form of radiopharmaceuticals which are injected inside human body for the diagnostic purposes or for the treatment to cure the disease. Various radiopharmaceuticals are selected in such way that they have short half-life of few days or weeks. They are well examined and established before being used as nuclear medicine. During the process, lot of studies are undertaken till they are being accepted as `radiopharmaceuticals' mainly for it's radiochemical purity and for the determinations of exact concentration as it is used directly

on human beings for the purpose of cure who are affected due to various health issues. The radiopharmaceuticals being used in India are $^{99m}$Tc, $^{131}$I, $^{32}$P, $^{51}$Cr, $^{153}$Sm, $^{90}$Y and $^{177}$Lu for the purpose of diagnosis and treatment for various types of cancers. India is one of the pioneers in the world to use $^{177}$Lu for it's therapeutical applications.

To acquire $^{177}$Lu by direct method, $^{176}$Lu target which is > 76% enriched is irradiated in the reactor. Due to high thermal neutron absorption cross section (2100 barns) of $^{176}$Lu, it gives the production of $^{177}$Lu with high specific activities (>20 Ci/mg) for receptor based radionuclide therapy using peptides and monoclonal antibodies. At present, the enriched $^{177}$Lu target is procured from the international market but efforts are going on to produce this enriched target material using laser induced electromagnetic separation technology in BARC. With increased demand for $^{177}$Lu over the years, few countries developed alternate technological methods for producing $^{177}$Lu via indirect irradiation methods involving $^{176}$Yb targets. Second alternative involves the separation of no-carrier-added (nca) $^{177}$Lu, where the specific activities achieved are near to the maximum theoretical specific activity (110 Ci/mg).

Lutetium-177 decays in 76% of events ($E_{\beta(max)}$ = 0.497 MeV) to the stable ground state of $^{177}$Hf with a half-life of 6.65 days and decays in 9.7% of events ($E_{\beta(max)}$ = 0.384MeV) and 12% of the time ($E_{\beta(max)}$ = 0.176 MeV) to an excited state of $^{177}$Hf that has 0.24967MeV) and 0.32132 MeV above the ground state, which de-excites to the ground state with the photon emission. During these radioactive decay events, $^{177}$Lu emits β- particles with an $E_{\beta(max)}$ of decay events, $^{177}$Lu emits β- particles with an $E_{\beta(max)}$ of 497 KeV (78.6%), 384KeV (9.1%) and 176KeV(12.2%) and low energy gamma photons [Eγ = 113 KeV (6.6%), 208 KeV (11%)].

During the production of $^{177}$Lu by direct route in a reactor, due to continuous irradiation $^{177}$Lu absorbs neutrons leading to the formation of $^{177/178}$Hf. The presence of $^{177/178}$Hf (IV) does not affect in the efficiency of $^{177}$Lu(III)- labelling reactions, but accumulation of hafnium atoms decreases the specific activity. Also $^{176m}$Lu ($T_{1/2}$ = 3.66h) and $^{177m}$Lu ($T_{1/2}$ = 160.4 d) are formed from $^{175}$Lu and $^{176}$Lu. $^{177m}$Lu with longer half-life poses problem from radioactivity point of view, hence is needed to be handled accordingly.

$^{177}$Lu is being used towards the preparation of complex,$^{177}$Lu DOTA-TATE(1,4,7,10-tetraazacyclodecane-14,7,10-tetraacetic acid coupled Tyr3-Octreotate) which is used for peptide receptor radionuclide therapy to cure patients suffering from various types of cancers. Quantitative determination of Lu becomes highly important for its effective application during medical therapy. $^{177}$Lu-labeled radiopharmaceuticals for peptide receptor radionuclide therapy (PRRT) involved administering of 7.4 GBq (200mCi i.e. 22.182 μg of $^{177}$Lu) per course for

the patient. It is bound to 180 to 300 μg of the peptide with the chelator DOTA, [DOTA0, Tyr3] octreotate[1-4].Technology for producing nca $^{177}$Lu has now been developed within BARC, Mumbai and is awaiting regulatory approval for clinical deployment.

Inductively Coupled Plasma – Atomic Emission Spectroscopic technique (ICP-AES) which scores over many techniques has been utilised for the determination of Lu during the present studies. It is well known that ICP-AES being multielemental technique has many advantages, namely, high sensitivity, reproducibility, accuracy, large linear dynamic range, practically no interferences and lower detection limits[5-7]. Due to these benefits, the technique is used in diversified fields including nuclear industry. In literature, some authors have reported the application of ICP-AES for the determination of $^{177}$Lu by ICP-AES[8-14]. Jeff D. Vervoot et. al have reported the isotopic composition of Yb and the determination of Lu concentrations and Lu/Hf ratios by isotope dilution using MC-ICPMS in geological samples at sub-ppm levels [15]. ICP-MS can be a better technique provided the instrument is modified suitably for the handling of radioactive Lutetium samples and also should be available at nearby site just after the preparation of $^{177}$Lu-DOTA-TATE sample, for analysis.

In our laboratory the commercial Jobin-Yvon ICP-AES instrument which was adapted in-house to glove box facility to analyse the radioactive samples for the determination of trace elements, being available nearby was used for the present studies[16]. Using this unit, we have reported the determinations of lanthanides, trace elements in HLW solutions, irradiated thoria bundle samples, radioactive aqueous dilute nitic samples containing Lu[17-18]. Using CCD based ICP-AES unit, we have reported the determination of trace elements including lanthanides in uranium, zirconium, thorium and lutetium matrices[19-22]. We had initiated and reported the determination of Lutetium by HR ICP-AES[23-24].The present studies were undertaken further on the similar lines and are described in detail here.

It is essential to determine the amounts of Lu in actual radiopharmaceutical samples accurately, as based on these values the final dose level to be administered to the patients was adjusted.The ICP-AES analysis results for Lu and Hf samples, were obtained for the actual samples received just before being transported to be administered for the patients, which were at sub-ppm levels. At such a low level, $^{177}$Hf does not compete in the radiolabeling of $^{177}$Lu-DOTAtate synthesis. But with higher amounts it does affect. Jose' de Souza Calderia had studied the interference of $^{177}$Hf, a decay product of $^{177}$Lu in the preparation of $^{177}$Lu-DOTAtate. The studies included the built up of $^{177}$Hf at various $^{177}$Lu$_{t1/2}$ values. The molar ratio of Lu-DOTAtate was calculated each day without considering the effect of $^{177}$Hf and

with consideration of $^{177}$Hf built up. The yield was found to be more when $^{177}$Hf influence was considered, which implies that $^{177}$Hf, a decay product of $^{177}$Lu, competes for the formation of the DOTA binding site. The author conclude that, these data will be relevant in the synthesis of the radiopharmaceuticals $^{177}$Lu-DOTAtate with high specific activity to be used in peptide receptor radionuclide therapy[24].

**Experimental:**

**Instrumentation**

All the experiments were performed using in-house glove box adopted JY Ultima high resolution inductively coupled plasma atomic emission spectrometer, the details of which have been given elsewhere[16].

**Reagents and Standard solutions**

Individual elemental stock solutions at 1 mg/ml each of Lu and Hf high purity (E-Merck, Darmstadt, Germany) were used for the studies. To prepare 0.5M $HNO_3$, Suprapur® (E-Merck) $HNO_3$ and distilled water re-distilled in quartz distillation unit were used. For profiling and for calibrations, 50μg/ml and 20μg/ml each of Lu and Hf were prepared after appropriate dilutions from stock solutions in 0.5M $HNO_3$.

Method

The determinations of Lu and $^{177}$Lu including Hf built up in actual radiopharmaceutical samples were carried out by ICP-AES. In our laboratory, the commercially procured Jobin-Yvon Ultima high resolution inductively coupled plasma – atomic emission spectrometer unit was suitably modified and was adopted to glove box to carry out the analysis of radioactive samples [10]. To be able to identify suitable analytical lines of Lu and Hf, 50 ppm each of individual solutions of Lu and Hf were aspirated into the plasma, while for calibration purposes, 0.5M $HNO_3$ and 20 ppm each of individual 20 ppm of Lu and Hf were used as low standard and high standard respectively. As the amounts of Lu in actual samples were expected at low levels, the calibration was limited to 20 ppm only and being pre-treated already, were analysed directly as received.

**Results and Discussion:**

**Peak Search and Profile of Spectral Lines of Lu and Hf**

For this purpose, 50 ppm of individual Lu and Hf were aspirated through the plasma under standardized plasma operating conditions followed by peak search, auto-attenuation and profile of the lines. For Lu, three analytical lines, viz., 261.542nm, 261.926nm and 264.14nm, while for Hf, 264.141nm and 282.022nm were selected for studies. Taking into account the intensity response (S/N) i.e. sensitivity and free from spectral interferences, the best analytical lines chosen for Lu and Hf were 261.542 nm and 282.022 nm respectively.

**Calibration of Lutetium and Hafnium**

The calibration curves were obtained using 20 ppm and 0.05 ppm individual solutions of Lu, Hf as high and low standards. In Table-2, intensity values for Lu and Hf were presented. Based on these values, the calibration curves for Lu 261.542 nm and Hf 282.022 nm were obtained and are shown in Fig.1. Detection limits for Lu and Hf were calculated as $(x+3\sigma)$, where `x' is the concentration equivalent to the average of intensity of blank solution at the specified wavelength and `$\sigma$' is the standard deviation of the blank measurements. The sensitivity was calculated based on the emission counts per concentration which is the slope of the calibration curve. The detection limits for Lu and Hf were 0.02mg/L and 0.07 mg/L respectively which are presented in Table-2 along with sensitivity values.

**Study of spectral interference of Hafnium on determination of Lutetium in dilute nitric acid medium**

Lu-177 isotope has a half-life of 6.65 days. This on storage builds up Hf in the samples to be used for medical purposes. Hence it was necessary to study the effect of Hf on the determination of Lu. The ICP-AES determination of Lu and Hf was performed using 261.542nm and 282.022nm analytical lines respectively. Though 282.022nm Hf line is wide apart from 261.542nm Lu line, and was not expected to interfere in the determination of Lu in presence of small quantities of Hf, but at higher levels of Hf built up after sufficient decay of ^{177}Lu, it will cause matrix interference on the determination of Lu at sub-ppm, few ppm levels by ICP-AES.

The amounts of Lu and Hf determined by ICP-AES were at sub-ppm levels. At the Lu concentration level of 0.05 µg/ml, the effect of Hf in the range of 0.05 µg/ml to 50 µg/ml was studied and the results are shown in Table – 3. It was found that even at 50 µg/ml level of

Hf, i.e., 1000 times that of the amount of Lu (at 0.05µg/ml), Lu determination was unaffected. One control sample of Lu at 0.65 µg/ml in presence of 16.67 µg/ml of Hf gave exact value of 0.65 µg/ml for Lu, which showed that this method has high accuracy with good precision. At such low levels, no inferences were observed.

## Analysis of real life samples by ICP-AES

Seven real life radiopharmaceutical samples were analysed for Lu contents by ICP-AES. For Lu, 261.542 nm analytical line being the most sensitive one, was used for this purpose. The final radiopharmaceutical products were expected to be highly pure with respect to no elemental impurities(non-radioactive) and also free from other radionuclide impurities, so ICP-AES analysis for Lu contents, beyond 50 µg/ml Hf and also for the determination of any other elemental impurities was not performed. These analyses results were obtained based on the requirements of the final product about to be administered to the patients, which were free from impurities but possibility of built up of Hf was expected due to transportation time. The results are shown in Table-4 and were found to be satisfactory with precision better than 2% RSD.

## Conclusions:

Using the developed method, it is possible to determine Lu in the range of 0.05-20 µg/ml by ICP-AES technique in presence of up to 50 µg/ml of Hf i.e. 1000 times that of the analyte without any spectral interferences with precision better than 2% RSD. The best emission lines chosen for Lu and Hf were 261.542 nm and 282.022 nm respectively. Subsequently, the analysis of the actual radio-pharmaceutical samples was carried out satisfactorily as was observed from the analysis data of control samples.

## Acknowledgement:

**Figure:**
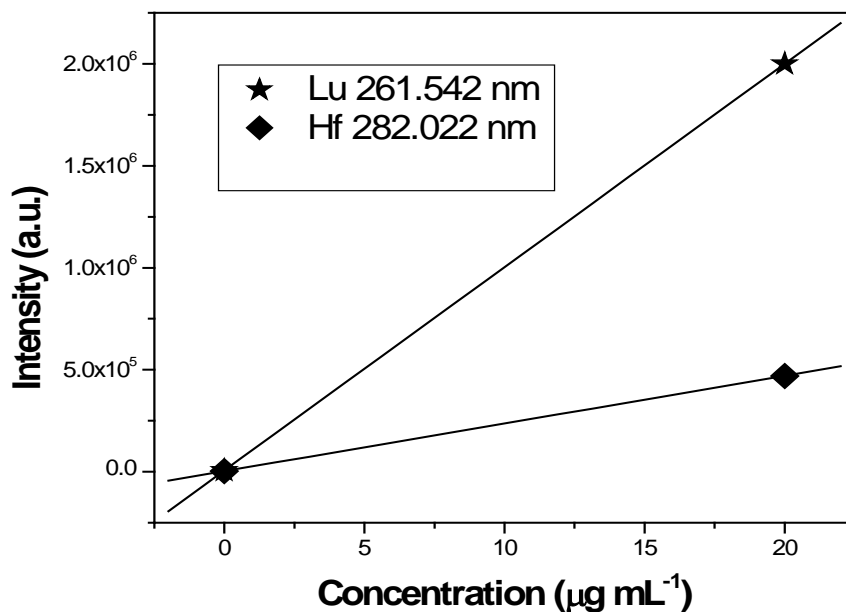


**Fig.1 Calibration curves for Lu and Hf**
**Lu: Slope= 99682;  Intercept=6354;  Regression coefficient $\chi^2 = 1$**
**Hf: Slope=23354;  Intercept=2907;  Regression coefficient $\chi^2 = 1$**

**Tables:**

**TABLE 1: Calibration (intensity) data for Lu and Hf**

| Solution | Lu 261.542nm | Hf 282.022nm |
|---|---|---|
| Std Blank (0.5M $HNO_3$) | 6354 | 2907 |
| Std. 1 (20 ppm Lu) | 2044660 | - |
| Std.2 (20 ppm Hf) | - | 469642 |

**TABLE 2  Detection limit, sensitivity for Lu and Hf**

| Element | Detection limit (mg/L) | Sensitivity (counts/mg/L) |
|---|---|---|
| Lu 261.542nm | 0.02 | $9.99 \times 10^4$ |
| Hf 282.022nm | 0.07 | $2.09 \times 10^4$ |

**TABLE – 3: Effect of Hf on Lu determination**

| Lu + Hf (µg/ml) Added | Lu (µg/ml) Estimated |
|---|---|
| 0.05+0.05 | 0.04 |
| 0.05+0.1 | 0.04 |
| 0.05+1 | 0.05 |
| 0.05+5 | 0.06 |
| 0.05+10 | 0.05 |
| 0.05+50 | 0.04 |
| 0.65+16.67 | 0.65 |

**TABLE–4 : ICP-AES analysis results for Lu in real samples**

| Sample | Conc. (µg/ml) |
|---|---|
| S-1 | 0.26 |
| S-2 | 0.13 |
| S-3 | 0.79 |
| S-4 | 0.11 |
| S-5 | 0.18 |
| S-6 | 0.09 |
| S-7 | 0.01 |

**REFERENCES**

1. Mathur and U. Pande, IANCAS Special Issue, NUCAR 2021, India, PP 23-26 (February 2022).

2. T. Das, Proceedings of DAE-BRNS 5th Symposium on Nuclear Analytical Chemistry (NAC-V), India, PP 59-60, (Jan. 2014).

3. A. Dash, M. Raghavan, A. Pillai and Furn F. Knapp Jr.,Nuclear Medicine and Molecular Imaging Volume 49, 85 (2015). US FDA – Reference ID: 4212675 (2018.)

4. S. Greenfield, I. LI. Jones and C.T. Bery, Analyst 89, 713 (1964).

5. R.H. Wendt and V.A. Fassel,Anal. Chem. 37(7), 920, (1965)

6. V.A. Fassel and R.N. Kniseley, Anal. Chem. 46, 13, 1110A (1974)

7. D. Pawlak, J. L. Parus, I. Sasinowska and R. Mikolajczak, J. of Radioanal. and Nucl. Chem., 261, 469, (2004).

8. C. Cutler, S. Wilder, M. Embree, H. Engelbrecht and A. Ketring, J. of Nucl. Medicine, 48 (supplement 2), 318 (May 2007).

9. U. Pandey, N. Gamre, Yogendra Kumar, P. Shetty, Haladhar Dev Sarma and A. Dash, J. of Radioanal. and Nucl. Chem. 307, 187 (2016).

10. M. Maiti, J. of Radioanal. and Nucl. Chem. 297, 319, (2013).

11. E.P. Horwitz, D.R. McAlister, A.H. Bond, R.E. Barrans, J.M. Williamson, Appl. Radiat. and Isotope 63, 23 (2005).

12. M. H. Maqsood, Asim Tameez Ud Din, A. H. Khan, Cureus: Open Access Review Article, Lahore, Pakistan 1, 30.01.2019.

13. DOI: 10.7759/cureus.3986

14. Yu Chao, Chao Liang, Yu Yang, Guanglin, Wang, Debabrata Maiti, Longlong Tian, Fei Wang, Wei Pan, Sang Wu, Kai Yong and Zhuang Liu, ACS Nano 12, 7519, (2018)

15. Jeff D. Vervoot, P. Jonathan Patchett, Ulf Soderlund, M. Baker, Geochemistry Geophysics Geosystems : An electronic journal of Earth Sciences Published by AGU and the Geochemical Society, Technical Brief 5(11), 2 ( 2004)

16. S.K., Thulasidas, Mithlesh Kumar, B.A. Dhawale, S.V. Godbole and V. Natarajan J. Instrum. Sci. Technology 43, 125, (2015).

17. S.K.Thulasidas, V.C.Adya, T.K.Seshagiri, Mithlesh Kumar, M.K.Bhide and S.V.Godbole, Atomic Spectroscopy 33(5), 158, (September/October 2012)

18. A.Sengupta, B. Rajeswari, V.C. Adya and R.M. Kadam Atomic Spectroscopy. 40(4), 127-132, (July/August 2019)

19. A.Sengupta, V.C. Adya and S.V.Godbole, J. of Radioanal. and Nucl. Chem. 298, 1117 (2013).

20. A.Sengupta, S.K.Thulasidas and V. Natarajan, Atomic Spectroscopy, 35(5), 213, (2014).

21. V.C.Adya, A.Sengupta, S.K.Thulasidas and V. Natarajan, Proceedings of Current Trends in Analytical Chemistry (CTAC-2015) conference, India (May 2015)

22. A. Sengupta, Y. Airan, S.K. Thulasidas, V. Natarajan, Atomic Spectroscopy. 36(2), 82, (March/April 2015).

23. K.V. Vimalnath, Priyalata Shetty, Sharad P. Lohar, V.C. Adya, S.K. Thulasidas, Sudipta Chakraborty, Ashutosh Dash,  J. Radioanal. Nucl. Chem. 302, 809, (2014).

24. José de Souza Caldeira Filho, J. Chem. Engg. 10,238, (2016)

# Assessment of Surface Water Quality by using Multivariate Statistical Techniques of Various Lakes of Kancheepuram District in Tamil Nadu, India

M.R. Kuppusamy[1] and T.M. Sridhar[2*]

1 Department of Chemistry, R. V. Govt.  Arts College, Chengalpattu – 603001,
2 Department of Analytical chemistry, University of Madras, Chennai-600025
*Email: tmsridhar23@gmail.com

**Abstract**

 Multivariate statistical methods such as Principal Component Analysis/Factor analysis (PCA/FA), and Cluster Analysis (CA) were used to characterize spatial and temporal variations and to find out the pollution source of 11 lakes of the Kancheepuram district, a northeast district of Tamilnadu in India. Sampling events were conducted during the northeast monsoon (Dec 2015 & 2016) and Pre-monsoon (Oct 2016). The 20 physicochemical water quality parameters were used to analyze the collected water samples. In PCA, four components were demonstrated up to 73.12% of the total variance in the data set. It clarifies that variations in water quality parameters concentration are mainly identified with agricultural, industrial, domestic wastes, and natural factors. The CA showed the formation of three clusters based on the water quality variation at different locations. From the CA data, sampling sites were classified into high, moderate, and least polluted. Among these sites, Kolavai, Nattapettai and Uthiramerur were highly polluted because of rapid urbanization and industrialization. Therefore, these areas need some effective measures to enhance the quality of water.

**Keywords:** Water quality, Physicochemical parameters, Statistical analysis, Lake water pollution.

## 1. Introduction:

 Water pollution is a worldwide issue and it reduces the accessible water resources. Making surface water to be contaminated is very easy compare to groundwater. Because of human activities and natural factors surface water was progressively defenseless. Lake water quality change is constantly directed by natural processes including weathering, precipitation, soil

erosion, etc., anthropogenic activities like agricultural, untreated urban sewage, industrial effluents, tourism, and the increased utilization of water resources[1] because of the multifaceted impacts noted previously, water purity degradation has become a difficult issue around the world. Remarkably in future freshwater resources may turn out to be rare, which would scare water resource use, particularly for drinking water and economic development. As indicated[2], roughly 1.1 billion people worldwide do not access a reliable source of drinking water. Lakes give the primary water resources for residential, industrial, and irrigational purposes; in any case, they are easily contaminated due to their critical roles in transporting from urban and industrial pollution and runoff from agricultural land. As a result of their critical roles in environmental and human health and monetary advancement, it is basic to prevent and control declining water quality in lakes. Therefore, solid data with regard to water quality parameter variations must be gathered for proper management; this has just been led in numerous nations and districts. Hence, research on lake water quality has become the exploration subject of numerous researchers over the world[3,4]. A few research works have been centered on the anthropogenic contamination of biological systems[5].

However, monitoring programs that provide representative and reliable information of the data are not effectively implemented because of both spatial and temporal variations in water quality including temperature, pH, substantial metals, harmful organic compounds, nutrients, and pesticides, etc. To secure water quality and to decrease the pressures on water resources, it is important to study elaborately on spatial-temporal variations in territorial water quality and identify the potential contamination sources. Recently, the multivariate statistical technique becomes suitable for a better understanding of water quality and environmental status, due to their capability to treat an enormous volume of spatial and temporal information from various monitoring sites[6-9].

In the research literature, different statistical techniques have been adopted which includes cluster analysis (CA)[10], PCA /factor analysis (FA)[11-12] and discriminate analysis (DA)[13] and were utilized for this kind of studies since they are capable to assess contaminations in water resources. Among these CA and PCA statistical techniques are fundamental tools to determine basic connections between the water quality parameters, predicting pollution sources, and group similar monitoring stations into clusters with similar characteristics[14]. Hence, in this work two statistical methods, PCA and CA were used to study the water quality in Kancheepuram district lakes, Tamilnadu. Kancheepuram is the first district in the

country with the largest number of lakes. It has more than 200 big lakes and ponds. In this study eleven main lakes of Kancheepuram were selected. They are Maduranthakam, Kolavai, Nattapettai, Uthukadu, Vaiyavoor, Thenneri, Uthiramerur, Edamichi, Pon Vilaintha *Kalathur, Chettipunyam, and Salavakkam Lakes. The samples were collected during northeast monsoon periods of December 2015 and 2016 and the southwest monsoon period of October 2016. Global warming is an event of climate change indicated by a general increase in average temperatures of the Earth, and that reshapes the weather balances and ecosystems for a long time[15].*

The 2015 urban flood resulted from heavy rainfall achieved by the annual northeast monsoon in November-December 2015[16,17]. Among the districts of Tamil Nadu, Kancheepuram district registered the heaviest rainfall of 183 percent higher at 181.5 cm as against average rainfall of 64 cm (The Hindu). Almost all the lakes reached their full storage capacity and some of the lakes had overflowed. Alike, in December 2016 an extremely Severe Cyclonic Storm Vardah was the fourth big cyclonic storm, just as the most extraordinary tropical cyclone of the 2016 North Indian Ocean cyclone season[18]. Cyclone Vardah made landfall near Chennai and it brought heavy rainfall to Kancheepuram, Chennai and Thiruvallur districts. But it is approximately three times less than the normal expected rainfall. The regular rain diminishes and water levels in lakes and reservoirs drop and then it tends to affect ecosystems. Due to climate changes, in recent decades summer season has extended up to October and at the same time shortage in rainfall takes place. Thus, in this part of the country there will be rainfall only for a couple of months. The sampling was carried out during 2015-16 and this data is relevant till date as there has been no major climate changes and sources of contamination are still prevalent.

## 2. Materials and Methods

### 2.1 Description of Study Area

Maduranthakam Lake is an artificial lake and is the biggest lake in the district of Kancheepuram and the second biggest lake in the state of Tamil Nadu. This Lake has an annual storage capacity of 694 Mcft and with a depth of 23.5 feet. It is spread over 1151.7 hectares and presently more than 30 villages are benefitted by this lake. The Maduranthakam Lake also receives water from the Kiliyar River which originates from Vandavasi Taluk of Thiruvannamalai District and municipal wastewater of Thiruvannamalai, Vandavasi, and Cheyyar enter into this lake through this river[19]. Kolavai Lake is the second biggest lake in

the Kancheepuram district and the tenth-biggest lake in the state of Tamil Nadu. Once a huge lake, Kolavai Lake has now decreased to a large portion of the size as a result of Mahindra World City which is built upon the bank of the lake. This Lake has an annual storage capacity of 476.69 Mcft and with a depth of 15.06 feet. It is spread over 894 hectares and presently above 12 villages are benefitted by this lake. It even supplies water to industries in Chennai when the lakes in Chennai go dry. The lake is currently being contaminated because of the rapid urbanization of Chengalpattu[20-21]. Nattapettai and Vaiyavoor were situated near to one another. Nattapettai Lake is a rain-fed freshwater lake used for irrigation and fishing. This lake also attracts a wide variety of migratory birds over the past few years. Nowadays, this lake gets contaminated because it receives municipal water from Thirukaalimedu and surrounding areas through Manjal neer kalvai. The main damages are caused by textile dyeing industries in Kancheepuram. Vaiyavoor lake water is utilized for household activities of Vaiyavoor and surrounding village people and both Nattapettai and Vaiyavoor lakes distribute water to farming fields. Uthukadu Lake is reduced to one-third part because this lake depends only on rainwater. Uthukadu Lake also distributes water to farming fields through irrigational canals. Thenneri Lake is one of the largest lakes in Kancheepuram. This lake provides water to surrounding villages[22]. Thenneri lake water joins with the Palar River at Chengalpattu through the Palar canal. Uthiramerur Lake is one of the famous lakes built during the Cholas period and is 1000 years old lake. This lake supplies water to farming fields and it is polluted by pharmaceutical, chemical, ceramic, fiberglass, and steel industries as well as domestic and agricultural waste. Edamichi, Pon Vilaintha *Kalathur, Chettipunyam, and Salavakkam are the small lakes situated in the village surrounded by farming fields. Edamichi, Pon Vilaintha Kalathur, Chettipunyam, and Salavakkam were the small lakes located in the town encompassed by cultivating fields and houses.*

## 2.2 Sample Collection and Analysis

Eleven sampling sites of different lakes were carefully selected to represent the nature of Kancheepuram district lakes and presented in Fig.1. Taking into account the variations of seasons two sampling events were conducted in a pre-monsoon (October 2016) and monsoon (December 2015 & December 2016) season. To estimate the effects of weather, some efforts were made to collect the samples in urban flood and vardah cyclone conditions. Water samples were manually collected approximately from the depth of 30 cm. The collected samples were stored in polyethylene bottles of previously soaked in 10% of $HNO_3$ for 24 h and rinsed several times with double distilled water and then they were rinsed with surface

water before sampling. The collected samples were acidified with 0.05M H$^+$ with nitric acid and stored at 4°C. Conductivity and pH of water samples were measured in situ at field sampling sites itself using a portable water quality analyzer (ELICO Model: PE138). After sampling all bottles were brought immediately to the college chemistry laboratory and stored in a refrigerator. The Collected samples were mainly utilized for in situ measurement of physicochemical characteristics and Water quality aspects[1,11,12,19]. Various physicochemical water quality parameters were analyzed using the standard analytical procedure following the standard methods (APHA-2012). The analytical methods followed for analysis of different parameters are given below in Table 1.

## 2.3 Multivariate Statistical Methods

Under the study to interpret the degree of association between two variables the Pearson correlation coefficient was obtained. PCA is generally applied to simplify the data by the removal of data noise using a dimensionality reduction technique and make it simpler to visualize by finding a set of principal components (eigenvectors). Principal Components (PC) are the orthogonal variables that are calculated by multiplying a list of coefficients with the correlated variables. FA was used to extract a lower-dimensional linear structure from a set of data and with regard provide a powerful means for detecting similarities among samples. FA can lower the contribution of less significant variables attained from PCA and further, that minimized the number of variables that have high loading on each factor using varimax rotation it is an orthogonal rotation method. The extracted group of variables is known as Varifactors[23]. CA is used to study similarities and dissimilarities between water samples. The classification of similar sampling sites into groups is illustrated by a dendrogram (tree diagram) and the reduction in the linearity of the original data leads to their proximity. CA was operated on the normalized data according to the Ward's method, by using the Squared Euclidean distances as a measure of similarity[24-25].

## 3. Results and Discussion

## 3.1 Statistical Analysis Results

Correlation is the linear relationship between two variable parameters. The linear relationship exists when an increase or decrease in the value of one variable is correlated with a corresponding increase or decrease in the value of the other variable. The correlation is reported as positive when the increase in one variable causes the increase in other and it is negative when the increase in one variable causes a decrease in the other. The correlation

coefficient has a value between +1 and -1 [26]. The correlation coefficient between various physicochemical water quality parameters was calculated and the values obtained were given in Table 2. The strong positive correlation occurred between Cl and Turb. (0.82), TH and Ca (0.91), $SO_4$ and Turb. (0.816), BOD (0.859). Pb and Cd (0.827) were found. The moderate positive correlation occurred between Turb. and Mg (0.774), K and Na (0.736), Turb. and EC (0.724), TDS (0.717). $SO_4$ and EC (0.781), TDS (0.776), Cl (0.785) were found. Other significant negative correlations occurred between pH and Turb. (-0.534), $SO_4$ (-0.539). Finally, Zn shows weakly negative correlations with variables except for pH (0.091) and DO (0.088) which shows weekly positive correlations.

### 3.2 Source identification of monitored parameters

The PCA/FA was dependent on the Pearson correlation matrix. It was used to understand the basic relationships between the various water quality parameters of all monitoring sites and to identify their unique properties. Principal components (PC) with Eigen values ≥ 1 considered as significant[27,28] so that four PCs with Eigen value greater than one only extracted as factor loadings. As indicated[29] factor loadings are classified as strong, moderate, and weak corresponding to >0.75, 0.75–0.5, and >0.5 respectively. The results given in Table3 which show that the four components of PCA analysis produced are explaining 73.12% of the total variance in the data set.

Among the four components, the first component (PC1) calculating that 29.71% of the total variance contained strong positive loadings of EC, TDS, Turb., BOD, Cl, and $SO_4$ corresponds to Group 1 in cluster analysis, moderate positive loadings of Na and K correspond to Group 2, strong negative loading of pH corresponds to Group 6 and other parameters show weakly positive and negative loadings. This strong positive loading is attributed to domestic sewage and agricultural waste[30]. Electrical conductivity is related to the concentration of conductive ions in the lake water. These conductive ions include dissolved salts and inorganic materials such as alkali metals, chlorides, sulfides, and carbonates. The strong positive loading of BOD representing organic pollution[31] is likely to arrive from dye industries in Kancheepuram. Na and K cations were originated from soil or rock structure by farming runoff.

The second component PC2, accounting for 19.96% of the total variance and it showed strong positive loading of Ca, Mg, TH, and TA corresponds to Group 4 and all other

parameters show weakly positive to negative loadings. The concentration of Ca and Mg shaped by anthropogenic factors and surface runoff. A high concentration of these increases the concentration of TH and TA. Alkalinity is water's ability to oppose acidic changes in the pH of the water using calcium and magnesium carbonates. But higher levels in lake water will affect aquatic life, farming irrigations patterns and livestocks.

The third component PC3 showed 15.22% of the total variance had strong to moderate positive loadings of Cr, Cd, Pb, Cu, and Fe and moderate negative loading of Zn. Among these Cd, Pb, and Cu experience Group 3 in cluster analysis, Cr and Fe undergo Group 5, and Zn corresponds to Group 6. Sources of these heavy metals[32,33] are agricultural, domestic sewage, pharmaceutical, and aquatic sources. Fe and Cr heavy metals were derived from lithogenic sources[34]. Higher concentrations of Fe are generally associated with organic matter of natural origin and leaching of soil and rocks. The fourth component PC4 revealed that 8.24% of the total variance and showed weak positive and weak negative loadings except DO. It showed strong negative loading and correspond to Group 6.

**3.3 Spatial and temporal variations in lake water quality**

CA was used to classify spatial and temporal similarity groups of all sampling sites by reported water quality similarities. The water quality similarities were categorized using factor loadings of physicochemical parameters and their cluster analysis is shown in Figure 2. The dendrogram of various sites obtained by Ward's method [35] in the pre-monsoon and monsoon seasons are shown in Figure 3. Temporal variations were noted in water quality parameters of studied lake water samples. Different parameters like EC, Td, BOD, Cl, TH, and TA showed maximum value during pre-monsoon, while minimum values were recorded during monsoon. The detected trends could be attributed to the evaporation of water from studied lakes during pre-monsoon and consequent dilution due to precipitation and runoff from catchment area during monsoon season.

The Spatial CA result revealed that all 11 sampling sites were classified into three clusters and sites in each cluster group hold similar water contaminations. The first group contained sites 1, 6, 8, 9, 10, and 11. These sampling sites are situated in zones with the highest agricultural runoff and domestic sewage activities, especially the dispersed and unsettled wastewaters from surrounding villages. Samples collected from these lakes were moderately polluted. The second group comprised of sites 2[36], 3, and 7. These sites were demonstrated at the highest level of pollution with multiple anthropogenic activities like an untreated waste,

industrial effluents, hospital waste, agricultural waste, domestic sewage, boating, and fishing activities. Group 3 contains 4 and 5 sampling sites respectively. These are the least contaminated sampling sites with agricultural activity.

## 4. Conclusion

This study enables us to identify the source of contamination effecting the water quality of Kancheepuram district lakes in Tamil Nadu, India. Multivariate statistical techniques were employed to characterize spatial and temporal variations of surface lake water quality data. The obtained values of some physicochemical water quality parameters at most sites showed that the average concentration exceeds the prescribed levels permitted by the Indian guidelines. Different parameters like EC, Turbidity, BOD, Cl, TH, and TA showed that maximum value during pre-monsoon, while minimum values were recorded during monsoon. The detected trends could be attributed to the evaporation of water from studied lakes during pre-monsoon and consequent dilution due to precipitation and runoff from catchment area during monsoon season. PCA for the four components indicates that 29.71%, 19.96%, 15.22% and 8.24% were obtained for PC1, PC2, PC3 and PC4 respectively for of the total variance which contained strong positive loadings. PCA/FA data has been used to bring out the relationship between various water quality parameters of all monitored sites. The results on factor loadings were classified as strong, moderate and weak respectively and based on this loadings water quality parameter classified into six groups in cluster analysis. The spatial cluster analysis result showed that 11 sampling sites were classified into three clusters with similar water contaminations. Among this, the second group contains highly polluted sites such as Kolavai, Nattapettai, and Uthiramerur lakes with multiple anthropogenic activities. The studies indicate that remedial measures have to be taken on a war footing to restore the water bodies from heavy metal contamination and prevent the sources of contaminants.
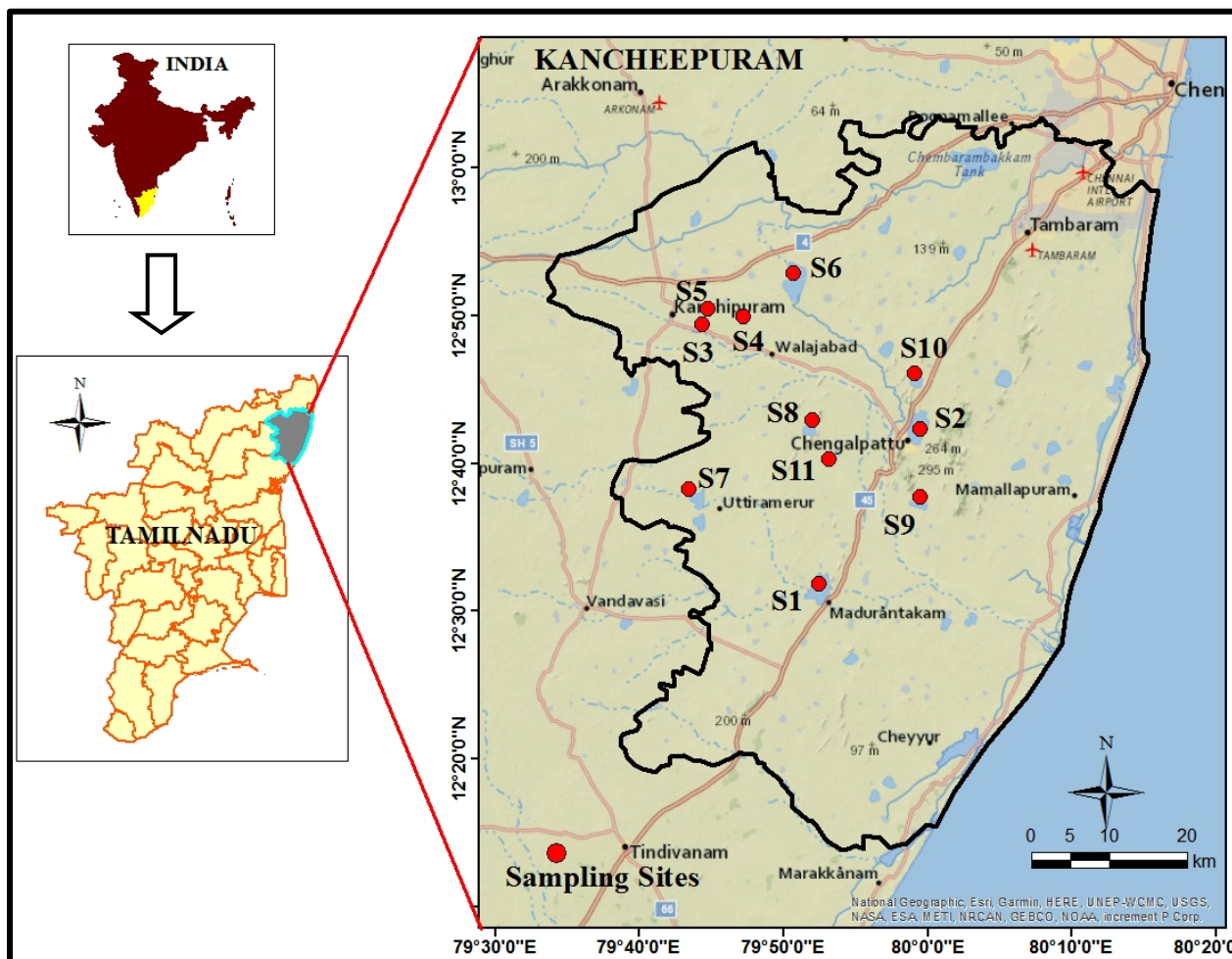
**Figures:**



**Figure 1: Location of sampling sites in Kancheepuram district lakes, India.**
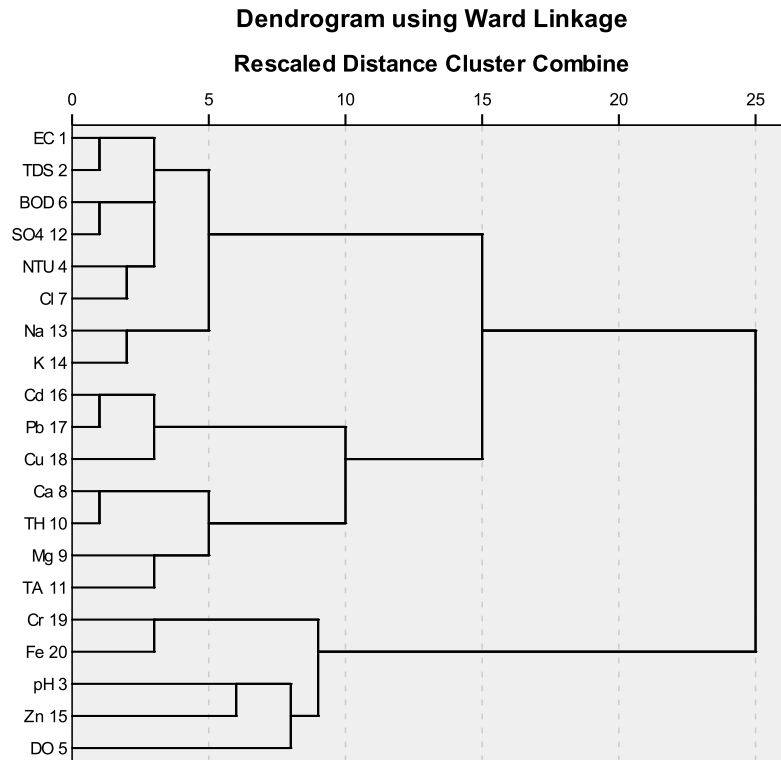
**Figure 2: Dendrogram showing clustering of water quality parameters.**
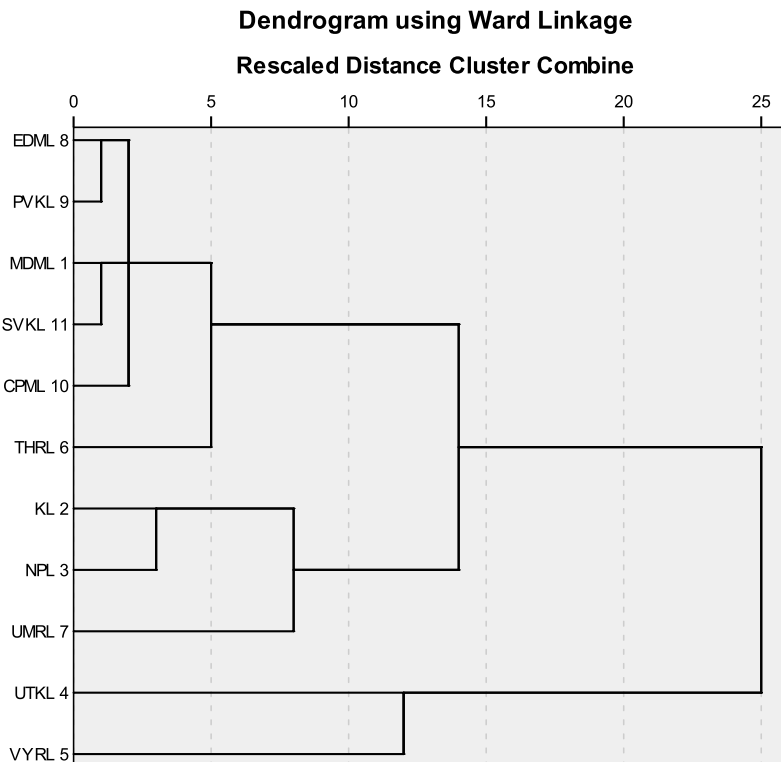


**Figure 3: Dendrogram showing clustering of sampling sites.**

**Tables:**

**Table1 : The water quality parameters and analytical methods used in this study.**

| Water quality parameters | Abbreviations | Units | Analytical Methods |
|---|---|---|---|
| Electrical Conductivity | EC | µS/cm | Portable conductivity meter |
| Total Dissolved Salts | TDS | mg/L | Conductivity TDS meter |
| pH | pH | - | Potentiometry/pH electrode |
| Turbidity | Turb. | NTU | Turbidimetry |
| Dissolved Oxygen | DO | mg/L | Winkler method |
| Biological Oxygen Demand | BOD | mg/L | Winkler method |
| Chloride | Cl | mg/L | Argentometric titration |
| Calcium | Ca | mg/L | EDTA titrimetric |
| Magnesium | Mg | mg/L | EDTA titrimetric |
| Total Hardness | TH | mg/L | EDTA titrimetric method |
| Total Alkalinity | TA | mg/L | Titrimetric |
| Sulphates | $SO_4$ | mg/L | Barium chloride |
| Sodium | Na | mg/L | Flame photometric |
| Potassium | K | mg/L | Flame photometric |
| Zinc | Zn | µg/L | ICP-AES |
| Cadmium | Cd | µg/L | ICP-AES |
| Lead | Pb | µg/L | ICP-AES |
| Copper | Cu | µg/L | ICP-AES |
| Chromium | Cr | µg/L | ICP-AES |
| Iron | Fe | µg/L | ICP-AES |

**Table 2: Pearson correlation coefficient matrix of physicochemical parameters for various lakes in Kancheepuram district.**

| | EC | TDS | pH | Turb. | DO | BOD | Cl | Ca | Mg | TH | TA | SO$_4$ | Na | K | Zn | Cd | Pb | Cu | Cr | Fe |
|---|---|---|---|---|---|---|---|---|---|---|---|---|---|---|---|---|---|---|---|---|
| **EC** | 1.000 | 1.000 | -0.341 | **0.724** | -0.379 | 0.680 | **0.799** | 0.671 | 0.335 | 0.628 | 0.495 | **0.781** | 0.491 | 0.486 | -0.113 | 0.445 | 0.265 | 0.344 | 0.076 | -0.122 |
| **TDS** | | 1.000 | -0.334 | **0.717** | -0.379 | 0.678 | **0.795** | 0.668 | 0.337 | 0.627 | 0.495 | **0.776** | 0.488 | 0.481 | -0.117 | 0.447 | 0.268 | 0.348 | 0.079 | -0.120 |
| **pH** | | | 1.000 | -0.534 | -0.149 | 0.475 | -0.406 | 0.097 | 0.213 | 0.025 | 0.162 | -0.433 | -0.328 | -0.375 | 0.091 | 0.026 | 0.004 | -0.134 | 0.191 | 0.214 |
| **Turb.** | | | | 1.000 | -0.185 | 0.631 | **0.820** | 0.495 | 0.229 | 0.455 | 0.240 | **0.816** | 0.629 | 0.606 | -0.164 | 0.407 | 0.321 | 0.405 | 0.053 | -0.075 |
| **DO** | | | | | 1.000 | -0.51 | -0.187 | 0.095 | -0.224 | -0.17 | -0.426 | -0.539 | -0.275 | -0.116 | 0.088 | -0.361 | -0.32 | 0.157 | 0.056 | 0.058 |
| **BOD** | | | | | | 1.000 | 0.629 | 0.271 | 0.257 | 0.306 | 0.358 | **0.859** | 0.656 | 0.585 | -0.146 | 0.306 | 0.226 | 0.120 | 0.073 | -0.111 |
| **Cl** | | | | | | | 1.000 | 0.665 | 0.304 | 0.610 | 0.357 | **0.785** | 0.451 | 0.587 | -0.067 | 0.353 | 0.233 | 0.271 | 0.021 | -0.119 |
| **Ca** | | | | | | | | 1.000 | 0.467 | **0.921** | 0.543 | 0.407 | 0.386 | 0.366 | -0.063 | 0.508 | 0.320 | 0.475 | 0.132 | -0.209 |
| **Mg** | | | | | | | | | 1.000 | **0.774** | 0.675 | 0.298 | 0.283 | 0.012 | -0.022 | 0.358 | 0.182 | 0.285 | 0.059 | -0.139 |
| **TH** | | | | | | | | | | 1.000 | 0.685 | 0.422 | 0.400 | 0.268 | -0.055 | 0.521 | 0.309 | 0.465 | 0.120 | -0.211 |
| **TA** | | | | | | | | | | | 1.000 | 0.367 | 0.421 | 0.281 | -0.119 | 0.486 | 0.381 | 0.129 | 0.112 | -0.114 |
| **SO$_4$** | | | | | | | | | | | | 1.000 | 0.528 | 0.505 | -0.14 | 0.395 | 0.246 | 0.191 | 0.025 | -0.066 |
| **Na** | | | | | | | | | | | | | 1.000 | **0.736** | -0.259 | 0.556 | 0.602 | 0.518 | 0.106 | -0.158 |
| **K** | | | | | | | | | | | | | | 1.000 | 0.000 | 0.246 | 0.351 | 0.187 | 0.010 | -0.029 |
| **Zn** | | | | | | | | | | | | | | | 1.000 | -0.244 | 0.194 | -0.276 | 0.187 | -0.101 |
| **Cd** | | | | | | | | | | | | | | | | 1.000 | **0.827** | 0.691 | 0.517 | -0.071 |
| **Pb** | | | | | | | | | | | | | | | | | 1.000 | 0.639 | 0.468 | -0.132 |
| **Cu** | | | | | | | | | | | | | | | | | | 1.000 | 0.443 | -0.105 |
| **Cr** | | | | | | | | | | | | | | | | | | | 1.000 | 0.662 |
| **Fe** | | | | | | | | | | | | | | | | | | | | 1.000 |

**Table 3: Factor loadings after varimax rotation of physicochemical parameters on four main components.**

| Parameters | PC 1 | PC 2 | PC 3 | PC 4 |
|---|---|---|---|---|
| EC | 0.764 | 0.461 | 0.096 | 0.126 |
| TDS | 0.758 | 0.462 | 0.100 | 0.128 |
| pH | -0.715 | 0.292 | 0.094 | 0.371 |
| Turb. | 0.855 | 0.179 | 0.196 | -0.091 |
| DO | -0.275 | -0.221 | -0.076 | -0.784 |
| BOD | 0.843 | 0.115 | 0.030 | 0.326 |
| Cl | 0.795 | 0.376 | 0.038 | -0.037 |
| Ca | 0.374 | 0.760 | 0.169 | -0.219 |
| Mg | 0.027 | 0.826 | 0.045 | 0.151 |
| TH | 0.279 | 0.908 | 0.140 | -0.091 |
| TA | 0.179 | 0.750 | 0.145 | 0.354 |
| $SO_4$ | 0.857 | 0.217 | 0.071 | 0.317 |
| Na | 0.643 | 0.206 | 0.445 | -0.042 |
| K | 0.724 | 0.025 | 0.179 | -0.051 |
| Zn | -0.132 | 0.067 | -0.518 | -0.050 |
| Cd | 0.236 | 0.455 | 0.744 | 0.048 |
| Pb | 0.199 | 0.261 | 0.766 | -0.024 |
| Cu | 0.195 | 0.322 | 0.707 | -0.473 |
| Cr | -0.138 | -0.013 | 0.836 | 0.200 |
| Fe | -0.172 | -0.355 | 0.585 | 0.410 |
| Eigen Value | 5.942 | 3.991 | 3.043 | 1.647 |
| Percent of variance | 29.709 | 19.955 | 15.217 | 8.235 |
| Cumulative percentage | 29.709 | 49.664 | 64.881 | 73.116 |

**References**

1.  M. M. Ali, M. L. Ali, M. S. Islam and M. Z. Rahman, Environ. Nanotech. Monitor. & Manag.,5, 27, 2016.

2.  Z. Wu, X. Wang, Y. Chen, Y. Cai, J. Deng, Sci. of the Tot. Environ., 612, 914, 2018.

3.  R. Kumar, A.S. Grover, M. Wats, Int. J. Recent Sci. Res., 9, 27831, 2018.

4.  Y. Zhao, Z. Yang, Y. Li, Procedia Environ. Sci., 2, 737, 2010.

5.  T. Koff, E. Vandel, A. Marzecova, E. Avi, A. Mikomagi, Int. J. Earth Sci., 4, 221,2016.

6.  S. Siddha and P. Sahu, Arabia. J. of Geosci., 15(12), 1, 2022.

7.  A. Barakat, M. Baghdadi, J. Rais, B. Aghezzaf, M. Slassi, Int. Soil Water Conserv. Res., 4, 284,2016.

8.  Y. Zhao, X. H. Xia, Z. F. Yang, F. Wang, Procedia Environ. Sci., 13, 1213, 2012.

9.  T. A. Basamba, K. Sekabira, C. M. Kayombo, P. Ssegawa, J. Environ. Stud., 22(2), 337, 2013.

10. E.A. Mohammad Salah, A.M. Turki, E.M. Al-Othman, J. Environ. Prot., 3, 1629, 2012.

11. M.R. Kuppusamy, V.V. Giridhar, Environ. Int., 32, 174,2006.

12. M.R. Kuppusamy, N. Mahalakshmi, R. Sureshkumar, C. Vanitha, Int. Res. J. Eng. Technol., 4, 1528, 2017.

13. H. Boyacioglu, Environ. Monit. Assess., 162, 15, 2010.

14. A. A. Uncumusaoglu, Global Nest J., 20,151, 2018.

15. S. YU. Schreider, D.I. Smith, A.J. Jakeman, Clim. Change., 47, 91,2000.

16. F. Rafiq, S. Ahmed, S. Ahmad, A.A. Khan, I. J. Sci. Eng. Res., 7(1), 721, 2016.

17. Archana Baghel, I.Conf. D.R.M. AGORA 2016. At Sohna, Haryana., 1-,2016.

18. M.P. Vasudha, G. Raju, Int. J. Appl. Eng. Res., 12, 12821,2017.

19. R. Arivarasi, M. Ganesan, Global Nest J., 19(1), 131, 2017.

20. A. Sonic Patritia, P. Martin, World J. Pharm. Res., 6, 1745, 2017.

21. N. Akila, Adv. Res. J. of Life Sci., 1(2,) 6, 2016.

22. T. Preeti, G.  Hariharan, G.R. Rajarajeswari, Water Environ. J., 30, 135, 2016.

23. U.N. Usman, M.E. Toriman, H. Juahir, M.G. Abdullahi, A.A. Rabiu, H. Isiyaka, Sci. and Tech., 4(3), 42, 2014.

24. A.S. Dawood, M.T. Jabbar, H.H. Al-Tameemi, and E.M. Baer, J. of Eco. Engg., 23(6), 189, 2022.

25. J. Ukpatu, E. Udoinyang, J.P. Udoh, Int. J. Geol. Agric. Environ., Sci. 3, 17, 2015.

26. P. Shroff, R.T. Vashi, V.A. Champaneri, K.K. Paatel, J. Fundam. Appl. Sci., 7(3), 340, 2015.

27. J.O. Kim, C.W. Mueller, Factor Analysis: Statistical Methods and Practical Issues, Quantitative Applications in the Social Sciences, Sage Publications, Beverly Hills, 07, 1978.

28. V. Panghal, P. Sharma, S. Mona, and R. Bhateria, Environ. Geochem. and Health., 1, 1, 2021.

29. C.W. Liu, K.H. Lin, Y.M. Kuo, Sci. Tot. Environ., 313, 77, 2003.

30. J. Badillo-Camacho, E. Reynaga-Delgado, I. Barcelo-Quintal, P.F. Zarate del Valle, U.J. López-Chuken, E. Eulogio Orozco-Guaren, J.I. AlvarezBobadilla. S. Gomez-Salazar, J. Environ. Prot., 6, 215, 2015.

31. X. Fan, B. Cui, H. Zhao, Z. Zhang, H. Zhang, Procedia Environ. Sci., 2, 1220, 2010.

32. Pankaj Bakshe and Ravin Jugade, Water Air Soil Pollut., 232, 78, 2021.

33. C. Zhang, Ecotoxic. and Environ. Saf., 139, 263, 2017.

34. F. Rakotondrabe, J.R.N. Ngoupayou, Z. Mfonka, E.H. Rasolomanana, A.J.N. Abolo, A.A. Ako, Sci. Total Environ., 610-611, 831, 2018.

35. J.H. Ward, J. Am. Stat. Assoc., 69, 236, 1963.

36. K. Ramesh babu, M. Selvanayagam, Int. J. Chem. Concept., 1, 15, 2015.

**A Booklet on Nuclear Analytical Techniques, Author: Dr. Nilima Shivadatta Rajurkar**

Dr. Raghaw Saran

Vice-President ISAS (India); Chief Advisor, J. ISAS; Adjunct Professor, RCOEMP Nagpur

saranraghaw@gmail.com
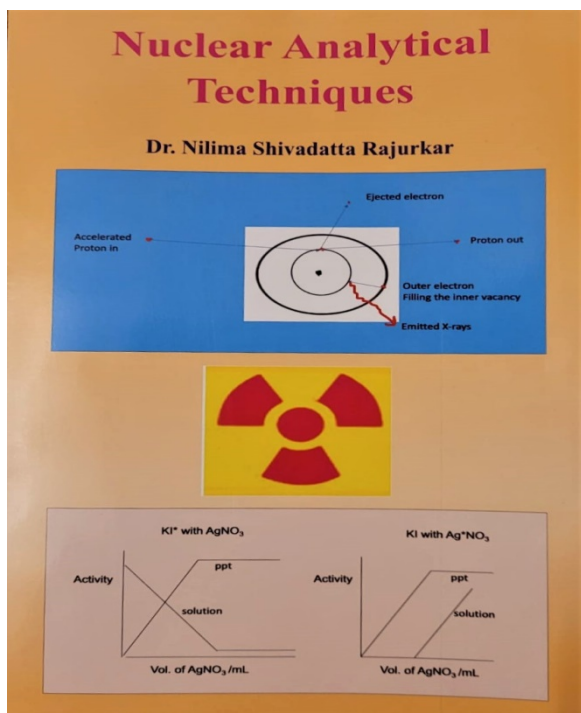
Nuclear analytical techniques (NAT) due to their multielement capability for the analysis of a variety of samples with a very low detection limits at nanogram to picogram levels (with almost no blank) for number of elements (depending upon the neutron flux) and sensitivities superior for some elements and comparable with many non-nuclear analytical techniques like F-AAS, hydride generation AAS, GF- AAS, ICP-OES and ICP-MS find vital role in trace elemental determinations. The techniques, being non-destructive and free from matrix interferences, have a tremendous potential to be used for a variety of samples, like art antiques, coins, forensic, archaeological specimens, semiconductors, environmental, lunar, etc.

In view of the characteristic features of NATs, a ready-made booklet consisting of various sub-branches of the technique with wider scope and immense utility in the analysis of variety of samples, authored by Dr Nilima S. Rajurkar has been published.

The booklet is quite handy and crisp which covers Neutron Activation Analysis (NAA), Particle Induced X-Ray Emission (PIXE), Isotope Dilution Analysis (IDA) and Radiometric Titrations (RT). It gives detailed information about the techniques in a simple, easily understandable language. The topics are  discussed on various aspects of the techniques, namely,  advantages, disadvantages, applications, limitations etc. with solved problems to have clear understanding of the concepts for each of the technique.

I am very confident that the booklet will be highly useful to the researchers as a ready-reckoner reference material, especially for upcoming students studying NAT.

The booklet is a recent publication (12.10.2022) by ISAS, Pune Chapter and is a low priced one with a meagre price of Rs 50/- , easily affordable and may be purchased from:

**Dr. Nilima S. Rajurkar,**

Chairperson, Pune Chapter.

nilima@rediffmail.com